

UCLA/2000/TEP/12
 MIT-CTP-2964
 hep-th/0003218
 March 2000

Near-extremal correlators and vanishing supergravity couplings in AdS/CFT

Eric D'Hoker^a, Johanna Erdmenger^b, Daniel Z. Freedman^{b,c} and Manuel Pérez-Victoria^{b*}

^a *Department of Physics
 University of California, Los Angeles, CA 90095*

^b *Center for Theoretical Physics
 Massachusetts Institute of Technology
 Cambridge, MA 02139*

^c *Department of Mathematics
 Massachusetts Institute of Technology
 Cambridge, MA 02139*

Abstract

We study near-extremal n -point correlation functions of chiral primary operators, in which the maximal scale dimension k is related to the others by $k = \sum_i k_i - m$ with $m \leq n - 3$. Through order g^2 in field theory, we show that these correlators are simple sums of terms each of which factors into products of lower-point correlators. Terms which contain only factors of two- and three-point functions are not renormalized, but other terms have non-vanishing order g^2 corrections.

We then show that the contributing AdS exchange diagrams neatly match this factored structure. In particular, for $n = 4, 5$ precise agreement in form and coefficient is established between supergravity and the non-renormalized factored terms from field theory. On the other hand, contact diagrams in supergravity would produce a non-factored structure. This leads us to conjecture that the corresponding bulk couplings vanish, so as to achieve full agreement between the structure of these correlators in supergravity and weak-coupling field theory.

*dhoker@physics.ucla.edu, jke@mitlns.mit.edu, dzf@math.mit.edu, manolo@pierre.mit.edu

1 Introduction

The AdS/CFT correspondence [1, 2, 3] has enabled the exact calculation of many correlation functions in a strong coupling limit of $\mathcal{N}=4$ $SU(N)$ supersymmetric Yang-Mills theory and to the initially surprising fact that many correlators appear to be non-renormalized—strong coupling results agree with free field limits. Although it is debatable whether a rigorous proof has been achieved, there is ample evidence from an interplay of arguments from AdS supergravity, order g^2 and g^4 calculations and formal non-perturbative considerations in the field theory that non-renormalization holds for all values of g and N and for general gauge groups.

This line of investigation is continued in the present paper in which we present new results on the structure of near-extremal n -point correlators. We consider the chiral primary operators $\mathcal{O}_k = \text{Tr}X^k$ and study order m sub-extremal n -point functions $\langle \mathcal{O}_k \mathcal{O}_{k_1} \cdots \mathcal{O}_{k_{n-1}} \rangle$ with $k = k_1 + \cdots + k_{n-1} - 2m$ and $0 \leq m \leq n - 3$. We shall call such correlators E_n^m functions. As we will review in more detail below, previous studies strongly suggest that (extremal) E_n^0 and (next-to-extremal) E_n^1 functions for $n \geq 3$ are not renormalized. On the field theory side these correlators are characterized by the factorization of their free-field graphs into products of two- and three-point structures. Order g^2 radiative corrections and Yang-Mills instanton corrections vanish [4, 5]. For $n \geq 4$ the contributing exchange diagrams from Type IIB supergravity on $AdS_5 \times S^5$ reproduce the factored space-time form, but contact diagrams involving quartic or higher order vertices do not. Thus supergravity E_n^0 and E_n^1 couplings should vanish, and this has been verified [6] for $n = 4$.

For near-extremality, $m \geq 2$, the situation is more complex as we now exemplify for the case $m = 2$. Here the E_4^2 correlator $\langle \mathcal{O}_2 \mathcal{O}_2 \mathcal{O}_2 \mathcal{O}_2 \rangle$ is known to be renormalized to order g^2 in field theory [7, 8] (for a recent calculation to three loops see [9]) and in the large N strong coupling limit in supergravity [10, 11, 12]. Indeed E_4^2 correlators have no special factored free-field limits, which suggests that one must examine E_5^2 functions to find non-renormalization. It is easy to see that the free-field graphs for the E_5^2 function $\langle \mathcal{O}_4 \mathcal{O}_2 \mathcal{O}_2 \mathcal{O}_2 \mathcal{O}_2 \rangle$ are of two distinct types; see Fig. 1. The first is a product of two three-point structures while the second is a product of a two-point and four-point structure. We show that the order g^2 radiative corrections to the first type vanish, but corrections to the second type do not vanish as might be expected because there is a four-point sub-structure present. Therefore the party is over as far as complete non-renormalization is concerned, but the factored structure is preserved by radiative corrections and this suggests that we look at the situation in supergravity.

Indeed it is very striking that the structure found at weak coupling is exactly mirrored at strong coupling in supergravity. In particular one of the two contributing double-exchange diagrams in supergravity reproduces the first factored structure of free field theory **both in space-time form and with exactly the same numerical strength**. The second double exchange and both single exchange diagrams reproduce the second factored struc-

ture from field theory, but contain a non-trivial four-point sub-structure which cannot be directly compared with weak coupling. Full agreement in structure between supergravity and weak field theory requires that the supergravity five-point coupling corresponding to the $s_4 s_2 s_2 s_2 s_2$ vertex vanishes. And indeed it must vanish for consistent decoupling of the multiplet containing the bulk field s_4 dual to \mathcal{O}_4 from the graviton multiplet. This is required by consistent Kaluza-Klein truncation of Type IIB supergravity on $AdS_5 \times S^5$, which means that the solutions to the equations of motion of $\mathcal{N}=8$ gauged supergravity on AdS_5 are exact solutions of the complete Type IIB supergravity theory on $AdS_5 \times S^5$ [13, 14]. This property forbids terms in the full action which both contain the graviton multiplet and are linear in a field of a higher Kaluza-Klein multiplet.

We show that the example of $\langle \mathcal{O}_4 \mathcal{O}_2 \mathcal{O}_2 \mathcal{O}_2 \mathcal{O}_2 \rangle$ generalizes to all E_5^2 functions (provided an extra assumption about descendent couplings holds). The factored structure of weak-coupling field theory agrees with supergravity calculations if all E_5^2 bulk couplings vanish, which is our prediction. There is a further extension of these results to all E_n^m functions with $m \leq n - 3$: Supergravity reproduces the factored space-time form of the field-theoretical calculation if bulk E_n^m couplings vanish. This leads us to conjecture that these couplings do indeed vanish.

We shall now give a detailed summary of the non-renormalization properties of $\mathcal{N}=4$ SYM correlators which have been established through study of the AdS/CFT correspondence.

1. *Two- and three-point functions of single-trace chiral operators.* The first result of this type came in [15] where a calculation of cubic couplings $g_{k_1 k_2 k_3}$ of the bulk fields s_k dual to the operators \mathcal{O}_k was combined with results [16] for AdS three-point integrals. Operators were normalized to have unit two-point functions, and it was observed that supergravity results for all three-point functions $\langle \mathcal{O}_{k_1} \mathcal{O}_{k_2} \mathcal{O}_{k_3} \rangle$ agreed with free field theory. This was soon followed by an explicit study of order g^2 radiative corrections in field theory which were shown to vanish for both two-point functions $\langle \mathcal{O}_k \mathcal{O}_k \rangle$ and three-point functions of non-normalized operators [17]. A superspace calculation may be found in [18]. Recently it was shown [19] that order g^4 contributions to $\langle \mathcal{O}_3 \mathcal{O}_3 \rangle$ vanish.

There have been many attempts to prove the non-renormalization of the three-point functions non-perturbatively in field theory. All approaches require unproved technical assumptions. Most convincing are the arguments using $\mathcal{N}=2$ analytic superspace [20, 21] that there are no possible superspace forms which could contribute to the derivative of a three-point function [22] with respect to the gauge coupling. (See also [23]).

2. *Two- and three-point functions of other chiral operators.* Related results have emerged from studies [24] of short representations [25] of the conformal superalgebra $SU(2, 2|4)$ of the $\mathcal{N}=4$ SYM theory. The chiral primaries \mathcal{O}_k are 1/2-BPS operators which transform in the $[0, k, 0]$ representation of the R -symmetry group $SU(4)$. There are other 1/2-BPS multitrace operators in the same representations, such as the projection of $: \text{Tr} X^{k_1} \text{Tr} X^{k_2} :$

in the $[0, k_1 + k_2, 0]$ representation, and all of them have protected dimension $\Delta_k = k$. It is therefore of interest to check the non-renormalization properties of these operators, and it was shown in [26] that order g^2 radiative corrections to their two- and three-point functions vanish for all gauge groups. The same question can be asked of the 1/4-BPS operators of dimension $p + 2q$ in the $SU(4)$ representation $[q, p, q]$ and the 1/8-BPS operators of dimension $p + 2q + 3r$ in the representation $[q, p, q + 2r]$. This is work in progress. See also [27, 28].

3. Extremal and next-to-extremal functions. The study of $E_n^{0,1}$ functions of chiral primaries for $n \geq 4$ emerged from a peculiarity of E_3^0 functions noted in [29]. It was shown that the factored form of free field theory was reproduced in supergravity as the product of a zero bulk coupling constant with an infinite AdS integral. The product was defined by analytic continuation in the dimensions Δ_k of the operators, and this procedure was justified in a related example by careful consideration of boundary interactions. It was then noticed [29] that E_n^0 functions had factored space-time forms for all $n \geq 4$. All contributing supergravity diagrams, each defined by analytic continuation, give the same factored form. The coefficient of this form could then be shown to vanish by OPE arguments. After order g^2 perturbative test in [4], non-perturbative $\mathcal{N} = 2$ and $\mathcal{N} = 4$ superspace arguments were given to support this result and to suggest that E_n^1 next-to-extremal correlators are not renormalized [30]. This was then shown for any n through order g^2 [5] and in AdS supergravity [5, 6].

4. Near-extremal functions. This brings us to the situation of E_n^m functions for $2 \leq m \leq n - 3$ which we have summarized at the beginning of this introduction with supporting arguments to be given below.

The paper is organized as follows. In Section 2 we present our results by considering the simplest possible case, which is the correlator $\langle \mathcal{O}_4 \mathcal{O}_2 \mathcal{O}_2 \mathcal{O}_2 \mathcal{O}_2 \rangle$. We then move on to general E_n^m functions, which we discuss from the field theory point of view in Section 3 and from the supergravity side in Section 4, paying particular attention to supergravity couplings in Section 5. There is a short conclusion and an Appendix which contains a detailed consideration of the AdS calculations essential to our argument.

2 The correlator $\langle \mathcal{O}_4 \mathcal{O}_2 \mathcal{O}_2 \mathcal{O}_2 \mathcal{O}_2 \rangle$

In order to illustrate the structure of E_n^2 correlation functions in the simplest possible situation, we study in detail the correlator $\langle \mathcal{O}_4(x) \mathcal{O}_2(x_1) \mathcal{O}_2(x_2) \mathcal{O}_2(x_3) \mathcal{O}_2(x_4) \rangle$. We first calculate the order g^2 corrections in SYM and then the corresponding diagrams in AdS supergravity. Although non-trivial radiative corrections appear at order g^2 , their factored form is compatible with supergravity provided the bulk $s_4 s_2 s_2 s_2 s_2$ coupling vanishes, as required by consistent Kaluza-Klein truncation.

2.1 $\langle \mathcal{O}_4 \mathcal{O}_2 \mathcal{O}_2 \mathcal{O}_2 \mathcal{O}_2 \rangle$ in SYM

We shall use the methods of [5] (where the interested reader can find more details). We normalize the operators as in [15]:

$$\mathcal{O}_k(x) = \frac{(2\pi)^k}{N^{k/2} \sqrt{k}} \text{Tr} X^k(x). \quad (2.1)$$

With this normalization the two point function is given by

$$\langle \mathcal{O}_k(x) \mathcal{O}_k(y) \rangle = \frac{1}{(x-y)^{2k}} \quad (2.2)$$

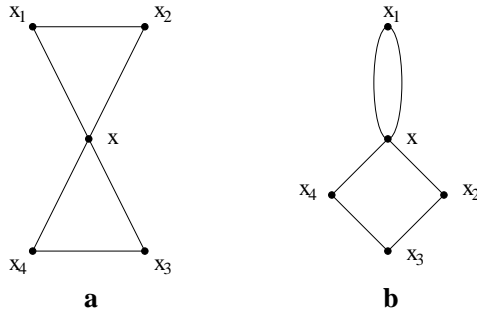


Figure 1: Feynman graphs contributing to the correlator $\langle \mathcal{O}_4 \mathcal{O}_2 \mathcal{O}_2 \mathcal{O}_2 \mathcal{O}_2 \rangle$ at the free-field level.

At the free-field level there are two connected graphs, up to permutations of the operators \mathcal{O}_2 (Fig. 1). Graphs *a* and *b* give the contributions

$$\begin{aligned} & \langle \mathcal{O}_4(x) \mathcal{O}_2(x_1) \mathcal{O}_2(x_2) \mathcal{O}_2(x_3) \mathcal{O}_2(x_4) \rangle_a \\ &= \mathcal{C}^{(a)} Q \frac{1}{(x-x_1)^2} \frac{1}{(x_1-x_2)^2} \frac{1}{(x_2-x)^2} \frac{1}{(x-x_3)^2} \frac{1}{(x_3-x_4)^2} \frac{1}{(x_4-x)^2}, \end{aligned} \quad (2.3)$$

$$\begin{aligned} & \langle \mathcal{O}_4(x) \mathcal{O}_2(x_1) \mathcal{O}_2(x_2) \mathcal{O}_2(x_3) \mathcal{O}_2(x_4) \rangle_b \\ &= \mathcal{C}^{(b)} Q \frac{1}{(x-x_1)^4} \frac{1}{(x-x_2)^2} \frac{1}{(x_2-x_3)^2} \frac{1}{(x_3-x_4)^2} \frac{1}{(x_4-x)^2}, \end{aligned} \quad (2.4)$$

respectively, where $\mathcal{C}^{(a,b)}$ are tensors in flavour space, and

$$\begin{aligned} Q &= \text{Str}(T^{a_1} \dots T^{a_4}) \text{Str}(T^{a_1} T^{a_2}) \text{Str}(T^{a_3} T^b) \text{Str}(T^b T^c) \text{Str}(T^c T^{a_4}) \\ &= \text{Str}(T^{a_1} \dots T^{a_4}) \text{Str}(T^{a_1} T^b) \text{Str}(T^b T^{a_2}) \text{Str}(T^{a_3} T^c) \text{Str}(T^c T^{a_4}) \\ &= \frac{N^2 - 1}{2^6}. \end{aligned} \quad (2.5)$$

The symmetric trace is defined as

$$\text{Str}(T^{a_1} \dots T^{a_k}) = \sum_{\text{perms } \sigma} \frac{1}{k!} \text{Tr}(T^{a_{\sigma(1)}} \dots T^{a_{\sigma(k)}}). \quad (2.6)$$

In the following we suppress explicit flavour tensors. Our order g^2 calculations are valid for all N , but for later comparison with supergravity, we write the large N limit of all non-vanishing contributions. Thus we have, for example, for the contribution of the graph a in Fig. 1,

$$\begin{aligned} & \langle \mathcal{O}_4(x) \mathcal{O}_2(x_1) \mathcal{O}_2(x_2) \mathcal{O}_2(x_3) \mathcal{O}_2(x_4) \rangle_a \\ &= \frac{4}{N} \langle \mathcal{O}_2(x) \mathcal{O}_2(x_1) \mathcal{O}_2(x_2) \rangle \langle \mathcal{O}_2(x) \mathcal{O}_2(x_3) \mathcal{O}_2(x_4) \rangle, \end{aligned} \quad (2.7)$$

where

$$\langle \mathcal{O}_2(x) \mathcal{O}_2(x_1) \mathcal{O}_2(x_2) \rangle = \frac{2\sqrt{2}}{N} \frac{1}{(x-x_1)^2 (x_1-x_2)^2 (x_2-x)^2}. \quad (2.8)$$

The coefficients in (2.7) and (2.8) incorporate both Wick combinatoric factors and the normalization factors of (2.1).

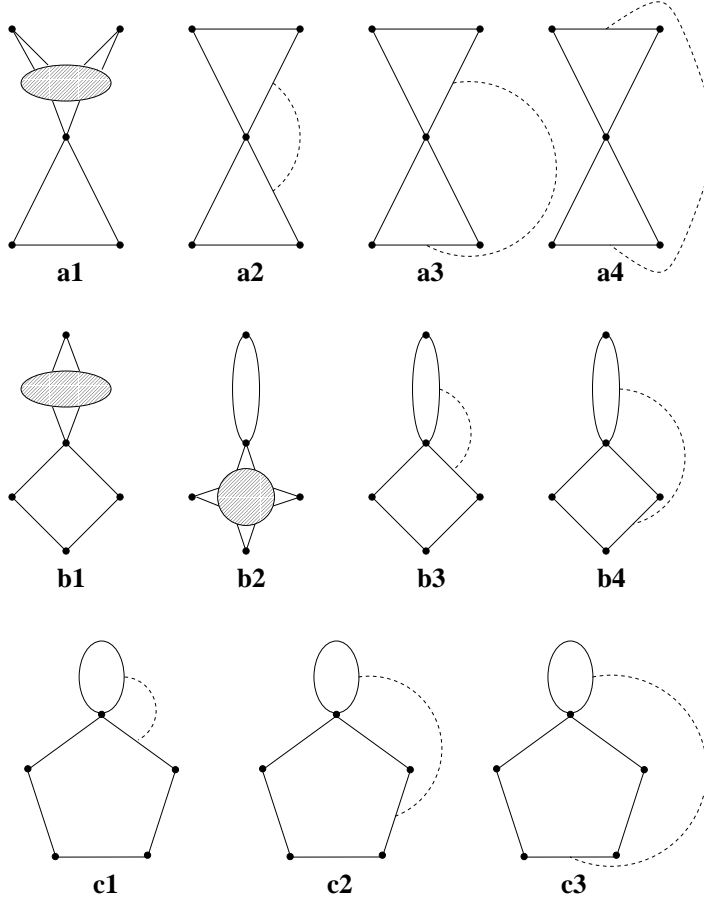


Figure 2: Graphs contributing to the correlator $\langle \mathcal{O}_4 \mathcal{O}_2 \mathcal{O}_2 \mathcal{O}_2 \mathcal{O}_2 \rangle$ at order g^2 .

Let us now consider the connected Feynman graphs contributing at order g^2 , which are depicted in Fig. 2. The dashed lines denote the combination of gauge boson exchanges and

quartic scalar interactions (see [5] for details). Graphs $a1$, $b1$ vanish due to the well-known non-renormalization theorems for the functions $\langle \mathcal{O}_2 \mathcal{O}_2 \rangle$ and $\langle \mathcal{O}_2 \mathcal{O}_2 \mathcal{O}_2 \rangle$. These theorems hold independently of colour contractions, see [26] and the further explanations below Eq. (13) in [5]. All the remaining graphs but $b2$ vanish due to the symmetry properties of colour indices. Let us show this explicitly for $a3$:

$$\begin{aligned}
a3 &\sim \text{Str}(T^{a_1} \dots T^{a_4}) \text{Str}(T^b T^c) \text{Str}(T^c T^{a_4}) \text{Str}(T^d T^{a_2}) \text{Str}(T^e T^{a_3}) \\
&\quad \cdot \left(A^{(a_3)} f^{a_1 b p} f^{d e p} + B^{(a_3)} f^{a_1 d p} f^{b e p} + C^{(a_3)} f^{a_1 e p} f^{b d p} \right) \\
&= \text{Str}(T^{a_1} \dots T^{a_4}) \left(A^{(a_3)} f^{a_1 a_4 p} f^{a_2 a_3 p} + B^{(a_3)} f^{a_1 a_2 p} f^{a_4 a_3 p} + C^{(a_3)} f^{a_1 a_3 p} f^{a_4 a_2 p} \right) \quad (2.9)
\end{aligned}$$

which vanishes as each term is a contraction of a symmetric with an antisymmetric tensor. Graphs $a2$, $a4$, $b3$, $b4$, $c1$, $c2$ and $c3$ can be shown to vanish in the same way. Therefore, the only possible contribution is that of graph $b2$, which factors into a two-point and a four-point function. For large N , the contribution of $b2$ is given by

$$\begin{aligned}
&\langle \mathcal{O}_4(x) \mathcal{O}_2(x_1) \mathcal{O}_2(x_2) \mathcal{O}_2(x_3) \mathcal{O}_2(x_4) \rangle_{b2} \\
&= \frac{4}{N} \langle \mathcal{O}_2(x) \mathcal{O}_2(x_1) \rangle \langle \mathcal{O}_2(x) \mathcal{O}_2(x_2) \mathcal{O}_2(x_3) \mathcal{O}_2(x_4) \rangle^{(1)}, \quad (2.10)
\end{aligned}$$

where the index (1) indicates order g^2 . We do not indicate the order in two- and three-point functions as they are not renormalized. The second factor was calculated and shown to contain logarithms in [7, 8, 9]. Therefore the full five-point correlator is renormalized at order g^2 . Nevertheless, the contribution does factor. Hence to order g^2 , the complete E_5^2 correlator is given by the sum of the two factored contributions (2.7) and (2.10),

$$\begin{aligned}
&\langle \mathcal{O}_4(x) \mathcal{O}_2(x_1) \mathcal{O}_2(x_2) \mathcal{O}_2(x_3) \mathcal{O}_2(x_4) \rangle \\
&= \frac{4}{N} \langle \mathcal{O}_2(x) \mathcal{O}_2(x_1) \mathcal{O}_2(x_2) \rangle \langle \mathcal{O}_2(x) \mathcal{O}_2(x_3) \mathcal{O}_2(x_4) \rangle \\
&\quad + \frac{4}{N} \langle \mathcal{O}_2(x) \mathcal{O}_2(x_1) \rangle \langle \mathcal{O}_2(x) \mathcal{O}_2(x_2) \mathcal{O}_2(x_3) \mathcal{O}_2(x_4) \rangle + \text{perms.} \quad (2.11)
\end{aligned}$$

The two-point and three-point structures are not renormalized. This factored space-time structure is a consequence of the properties of $\mathcal{N} = 4$ SYM. Conformal invariance alone permits a more general structure.

2.2 $\langle \mathcal{O}_4 \mathcal{O}_2 \mathcal{O}_2 \mathcal{O}_2 \mathcal{O}_2 \rangle$ in AdS

According to the Maldacena conjecture, the same function can be calculated (at strong coupling and large N) using classical Type IIB supergravity on $AdS_5 \times S^5$. The corresponding connected Witten diagrams are shown in Fig. 3, up to permutations. We refer to the bulk fields dual to the operator \mathcal{O}_k as s_k . There are double-exchange (a and b), single-exchange (c and d) and contact diagrams (e). The cubic and quartic couplings we

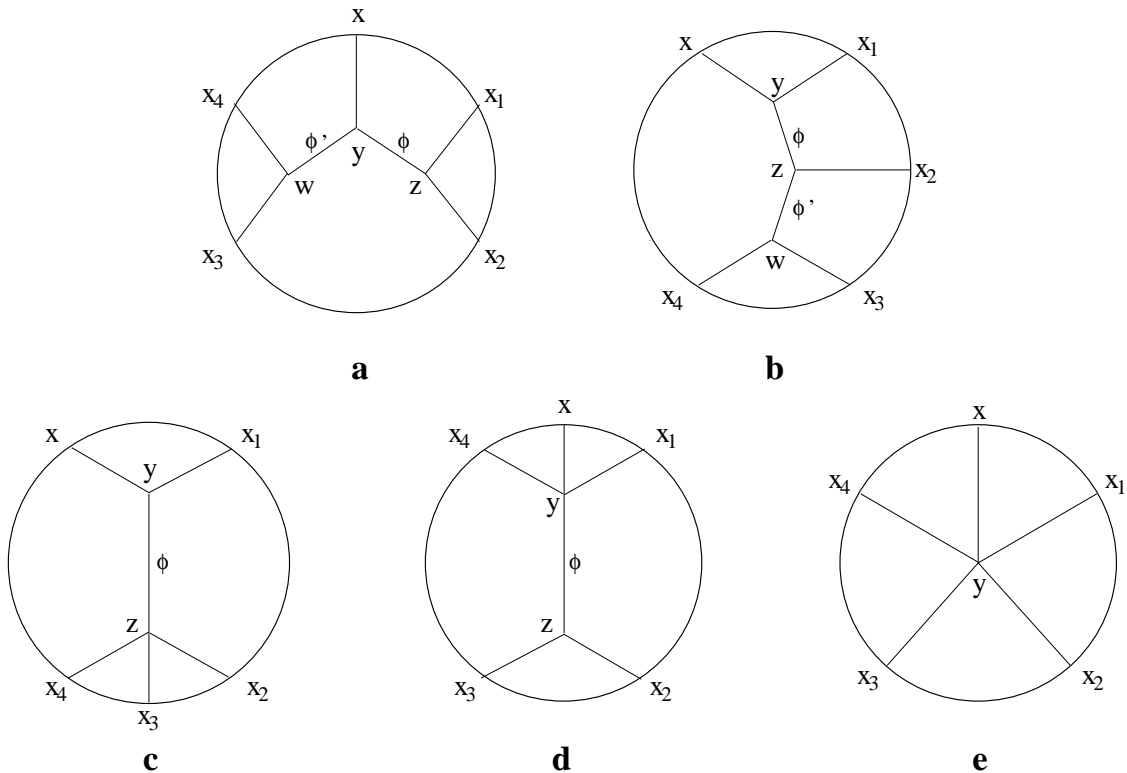


Figure 3: Witten diagrams contributing to E_5^2 correlators in the AdS/CFT correspondence.

need were calculated in [15, 31, 32] and [33], respectively. The main property we need for our purposes is that the couplings of the vertices $s_2s_2s_4$, $s_2s_2s_2s_6$ and $s_2s_2s_2s_4$ vanish (although allowed by $SU(4)$ symmetry). By “vanishing coupling” we mean that the combination of derivative and non-derivative terms in the vertex give a vanishing net coupling in the bulk. It is important to note that even if the coupling vanishes in the bulk, there can be a contribution from a surface term if the space-time integral is divergent [29]. In [29] it was shown (for a particular case) that this boundary contribution is also obtained when couplings and integrals are regularized by analytic continuation. Moreover, analytic continuation has successfully produced results which agree with field theory [15, 29, 5]. We use this method here as well and regularize the divergent integrals by analytic continuation in the highest conformal dimension, $k = \Delta = 4 \rightarrow 4 - \varepsilon$, which also implies that the vanishing couplings give rise to factors of ε .¹ The convention of normalized two-point functions [15] requires that AdS integrals must be divided by a product of factors

$$\mathcal{N}_k = \frac{4N}{\pi^2} \frac{1}{2^{k/2}} \frac{\sqrt{k}(k-1)(k-2)}{(k+1)}, \quad k > 2,$$

¹An alternative procedure would be to analyze the implications of field redefinitions removing the surface terms, in the spirit of [6].

$$\mathcal{N}_2 = \frac{4N}{\pi^2} \frac{1}{\sqrt{2} \cdot 3}, \quad (2.12)$$

one for each external s_k line². For the couplings \mathcal{G} we also use the expressions given in [15], and the Poisson kernels $K_k(x, z)$ are given in the Appendix.

Let us first consider the exchange of primary fields. We begin with diagram a . The exchanged fields ϕ, ϕ' have to be in the representation with Dynkin labels $[0, \delta, 0], [0, \delta', 0]$, respectively, with δ, δ' restricted to 2 and 4 in the present example. The contribution of the exchange diagram for generic δ, δ' is given by

$$\begin{aligned} & \langle \mathcal{O}_4(x) \mathcal{O}_2(x_1) \mathcal{O}_2(x_2) \mathcal{O}_2(x_3) \mathcal{O}_2(x_4) \rangle_a \\ &= \frac{\mathcal{G}(4, \delta, \delta') \mathcal{G}(\delta, 2, 2) \mathcal{G}(\delta', 2, 2)}{\mathcal{N}_4 \mathcal{N}_2^4} \iiint \frac{d^5 y}{y_0^5} \frac{d^5 z}{z_0^5} \frac{d^5 w}{w_0^5} K_4(x, y) G_\delta(y, z) \\ & \quad \cdot K_2(x_1, z) K_2(x_2, z) G_{\delta'}(y, w) K_2(x_3, w) K_2(x_4, w). \end{aligned} \quad (2.13)$$

If $\delta = \delta' = 2$, the vertex y is extremal, such that the corresponding coupling vanishes [15],

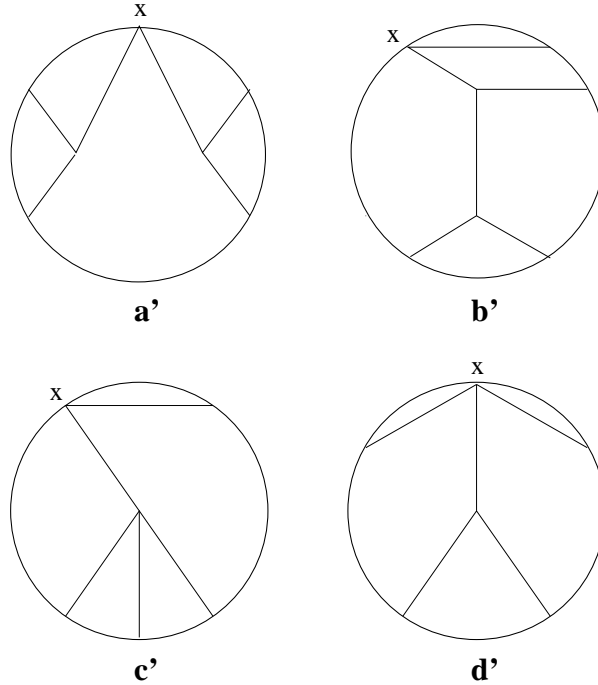


Figure 4: Non-vanishing contributions to E_5^2 functions in AdS supergravity. Diagram d' does not appear for $\langle \mathcal{O}_4 \mathcal{O}_2 \mathcal{O}_2 \mathcal{O}_2 \mathcal{O}_2 \rangle$.

and it is adjacent to the boundary operator with the highest conformal dimension. It is crucial to note here and for the subsequent discussion that in this case the integral over y

²The normalization for $k = 2$ is in agreement with the discussion in [34].

is divergent, with the dominant contribution arising when $y \sim x$. As shown in detail in the Appendix, using analytic continuation $\Delta \rightarrow \Delta - \varepsilon$ for the highest conformal dimension, both for the extremal coupling and to evaluate the y integral, we find an unambiguous finite expression for $\varepsilon \rightarrow 0$.

The remaining integrals over z and w are finite and, as represented in diagram a' of Fig. 4, factor into two three point functions

$$\langle \mathcal{O}_2(x)\mathcal{O}_2(x_1)\mathcal{O}_2(x_2) \rangle = \frac{\mathcal{G}(2, 2, 2)}{\mathcal{N}_2^3} \int \frac{d^5 z}{z_0^5} K_2(x, z)K_2(x_1, z)K_2(x_2, z), \quad (2.14)$$

which may be evaluated using [16] with the result

$$\langle \mathcal{O}_2(x)\mathcal{O}_2(x_1)\mathcal{O}_2(x_2) \rangle = \frac{2\sqrt{2}}{N} \frac{1}{(x-x_1)^2(x_1-x_2)^2(x_2-x)^2}. \quad (2.15)$$

Putting all the factors together and inserting the explicit values for the supergravity couplings, we obtain for the five-point function contribution (2.13)

$$\begin{aligned} & \langle \mathcal{O}_4(x)\mathcal{O}_2(x_1)\mathcal{O}_2(x_2)\mathcal{O}_2(x_3)\mathcal{O}_2(x_4) \rangle_a \\ &= \frac{4}{N} \langle \mathcal{O}_2(x)\mathcal{O}_2(x_1)\mathcal{O}_2(x_2) \rangle \langle \mathcal{O}_2(x)\mathcal{O}_2(x_3)\mathcal{O}_2(x_4) \rangle, \end{aligned} \quad (2.16)$$

which is in **exact agreement in form and value** with the free-field contribution (2.7). Later we show that this is valid for general conformal dimensions as well, not only in the simple case considered here as an introduction. This is both a non-trivial test of the AdS/CFT correspondence and of the method of analytic continuation. Of course this explicit comparison is possible since the three point functions involved are not renormalized, and there is exact agreement of the functional form between weak and strong coupling. As far as the factors are concerned, we see that the field theory large N Wick factors agree with the factors obtained from the supergravity couplings, the normalization of the propagators and the integral evaluated using analytic continuation.

If $\delta + \delta' > 4$ in (2.13), at least one of the remaining vertices is extremal and its coupling vanishes. The integral, however, is finite and hence the diagram vanishes.

Let us now consider diagram b , where the exchanged field ϕ has to be in the representation $[0, \delta, 0]$ with $\delta = 2, 4, 6$ and conformal dimension δ . If $\delta = 2$, the cubic vertex at y is again extremal and the corresponding coupling vanishes. Again, there is a zero-times-infinity situation, such that a finite contribution emerges from the region $y \sim x$:

$$\begin{aligned} & \langle \mathcal{O}_4(x)\mathcal{O}_2(x_1)\mathcal{O}_2(x_2)\mathcal{O}_2(x_3)\mathcal{O}_2(x_4) \rangle_b \\ &= \frac{1}{\mathcal{N}_4\mathcal{N}_2^4} \sum_{\delta'=2,4} \mathcal{G}(4, 2, 2)\mathcal{G}(\delta', 2, 2)\mathcal{G}(\delta', 2, 2) \iiint \frac{d^5 y}{y_0^5} \frac{d^5 z}{z_0^5} \frac{d^5 w}{w_0^5} K_4(x, y)K_2(x_1, y) \\ & \quad \cdot G_2(y, z)K_2(x_2, z)G_{\delta'}(z, w)K_2(x_3, w)K_2(x_4, w) \end{aligned}$$

$$\begin{aligned}
&= \frac{2\sqrt{2}}{N} \langle \mathcal{O}_2(x) \mathcal{O}_2(x_1) \rangle \frac{1}{\mathcal{N}_2^3} \sum_{\delta'=2,4} \mathcal{G}(\delta', 2, 2) \mathcal{G}(\delta', 2, 2) \\
&\quad \cdot \iint \frac{d^5 z}{z_0^5} \frac{d^5 w}{w_0^5} K_2(x, z) K_2(x_2, z) G_{\delta'}(z, w) K_2(x_3, w) K_2(x_4, w) \\
&= \frac{4}{N} \langle \mathcal{O}_2(x) \mathcal{O}_2(x_1) \rangle \langle \mathcal{O}_2(x) \mathcal{O}_2(x_2) \mathcal{O}_2(x_3) \mathcal{O}_2(x_4) \rangle_b. \tag{2.17}
\end{aligned}$$

Again there is agreement between the factors in (2.17) and in (2.10). However since the four-point functions are renormalized, it is not possible to compare them directly: In (2.10) we have an order g^2 contribution at weak coupling, whereas in (2.17) we have an exchange contribution at strong coupling. Diagram b' of Fig. 4 represents the space-time structure of Eq. (2.17). The integrals on z and w are finite.

If $\delta = 4$ (such that the vertex at y is next-to-extremal), the field ϕ' is in the representation $[0, \delta', 0]$ with $\delta' = 2$ or $\delta' = 4$. Then either the vertex at z or the vertex at w is extremal and hence has a vanishing coupling. If $\delta = 6$, the only possibility is $\delta' = 4$ and the three vertices are extremal. On the other hand, as shown in the Appendix, the integrals are finite in all these cases. Therefore the corresponding diagrams vanish.

The four-point factor in (2.17) corresponds to an exchange diagram. In diagram c we can have $\delta = 2, 4, 6$. If $\delta = 2$ the vertex y is extremal and the diagram factors:

$$\begin{aligned}
&\langle \mathcal{O}_4(x) \mathcal{O}_2(x_1) \mathcal{O}_2(x_2) \mathcal{O}_2(x_3) \mathcal{O}_2(x_4) \rangle_c \\
&= \frac{2\sqrt{2}}{N} \langle \mathcal{O}_2(x) \mathcal{O}_2(x_1) \rangle \mathcal{G}(2, 2, 2, 2) \int \frac{d^5 z}{z_0^5} K_2(x, z) K_2(x_2, z) K_2(x_3, z) K_2(x_4, z) \\
&= \frac{4}{N} \langle \mathcal{O}_2(x) \mathcal{O}_2(x_1) \rangle \langle \mathcal{O}_2(x) \mathcal{O}_2(x_2) \mathcal{O}_2(x_3) \mathcal{O}_2(x_4) \rangle_c, \tag{2.18}
\end{aligned}$$

where the four-point function is the contact contribution to the E_4^2 function. The factored structure is shown in diagram c' of Fig. 4. If $\delta = 4$ there is a next-to-extremal quartic vertex at z . The diagram gives zero since the z -integral is finite (Appendix) and the coupling vanishes. If $\delta = 6$ both vertices have vanishing couplings as they are extremal and the integral is finite, so the diagram vanishes as well.

In diagram d both $\delta = 2, 4$ are possible. In both cases the vertex at y is sub-extremal and the integral finite. If $\delta = 2$, the quartic coupling at y is next-to-extremal and has a vanishing coupling. If $\delta = 4$ both vertices are extremal and have vanishing couplings. Therefore this diagram does not contribute.

Let us now study the same set of diagrams when $SU(2, 2|4)$ descendants are exchanged. We will show that descendent contributions to diagrams $a - d$ of Fig. 3 all vanish or give corrections to the four-point structure in (2.17). Since the discussion is very technical, the reader interested only in the main flow of the argument may wish to proceed to the summary paragraph below.

$SU(4)$ flavour symmetry restricts the quantum number of internal lines according to the Clebsch-Gordan decomposition ($q \leq k$)

$$[0, k, 0] \otimes [0, q, 0] = \bigoplus_{\mu=0}^q \bigoplus_{\nu=0}^{q-\mu} [\nu, k+q-2\mu-2\nu, \nu]. \quad (2.19)$$

In the present application $[0, k, 0]$ and $[0, q, 0]$ are external chiral primary fields dual to operators of dimension k and q , respectively, while the exchanged fields in representations $[\nu, j, \nu]$ on the right side are either primaries (for $\nu = 0$) of dimension $\Delta_\phi = j$ or descendants (for $\nu \geq 0$) of dimension $\Delta_\phi > j + 2\nu$. A descendent must descend from a chiral primary in the representation $[0, l, 0]$ with $\Delta_\phi > l \geq j + 2\nu$.

We shall also use a fact which follows from the unique representation of given three-point function as an extended superspace invariant. All component bulk couplings $s_k s_q \phi$, $s_k s_q \phi'$, $s_k \phi \phi'$ are then related by extended supersymmetry to those of the scalar primaries in the same multiplet, $s_k s_q \tilde{s}$, $s_k s_q \tilde{s}'$, $s_k \tilde{s} \tilde{s}'$, where \tilde{s} and \tilde{s}' are the chiral primaries from which ϕ and ϕ' descend. In particular, descendent couplings vanish if the associated primary vertex vanishes because of extremality. The final link of our argument is the convergence or divergence of the AdS integrals, as discussed in the Appendix.

We start with diagram b , where $SU(4)$ symmetry allows the combinations of exchanged fields ϕ , ϕ' in the following representations:

$$\begin{aligned} \phi = [0, 2, 0] &\rightarrow \phi' = [0, 0, 0], [0, 2, 0], [1, 0, 1], [0, 4, 0], [1, 2, 1], [2, 0, 2] \\ \phi = [0, 4, 0] &\rightarrow \phi' = [0, 2, 0], [0, 4, 0], [1, 2, 1] \\ \phi = [1, 2, 1] &\rightarrow \phi' = [0, 2, 0], [1, 0, 1], [0, 4, 0], [1, 2, 1], [2, 0, 2] \\ \phi = [0, 6, 0] &\rightarrow \phi' = [0, 4, 0] \\ \phi = [1, 4, 1] &\rightarrow \phi' = [0, 4, 0], [1, 2, 1] \\ \phi = [2, 2, 2] &\rightarrow \phi' = [0, 4, 0], [2, 0, 2] \end{aligned} \quad (2.20)$$

If ϕ is a chiral primary in the $[0, 2, 0]$, while ϕ' is any descendent, the exchange diagrams are infinite and made finite by analytic continuation of the highest dimension $4 \rightarrow 4 - \varepsilon$ both in the integrand and in the vanishing extremal coupling. The limit $\varepsilon \rightarrow 0$ reduces all diagrams to b' of Fig. 4 and results in a correlation function of the structure (2.17), *i.e.*, the product of the two-point function $\langle \mathcal{O}_2 \mathcal{O}_2 \rangle$ and a radiatively corrected four-point function $\langle \mathcal{O}_2 \mathcal{O}_2 \mathcal{O}_2 \mathcal{O}_2 \rangle$. In all other cases in (2.20), ϕ has scale dimension $\Delta_\phi > 2$, and the AdS integral is finite. On the other hand at least one of the couplings vanishes because the associated primary vertex is either extremal or forbidden by $SU(4)$ symmetry.

For descendants in diagram a of Fig. 3, the allowed representations are

$$\begin{aligned} \phi = [0, 0, 0] &\rightarrow \phi' = [0, 4, 0] \\ \phi = [0, 2, 0] &\rightarrow \phi' = [0, 2, 0], [0, 4, 0], [1, 2, 1] \\ \phi = [1, 0, 1] &\rightarrow \phi' = [1, 2, 1], [0, 4, 0] \\ \phi = [0, 4, 0] &\rightarrow \phi' = [0, 0, 0], [0, 2, 0], [1, 0, 1], [0, 4, 0], [1, 2, 1], [2, 0, 2] \\ \phi = [1, 2, 1] &\rightarrow \phi' = [0, 2, 0], [1, 0, 1], [0, 4, 0], [1, 2, 1], [2, 0, 2] \\ \phi = [2, 0, 2] &\rightarrow \phi' = [0, 4, 0], [1, 2, 1], [2, 0, 2] \end{aligned} \quad (2.21)$$

The case where ϕ and ϕ' are chiral primaries in the $[0, 2, 0]$ is the no-descendent case considered above. In all other cases $\Delta_\phi + \Delta_{\phi'} > 4$ and the integrals are finite, while at least one of the (associated) couplings is extremal and vanishes. Hence there are no descendent contributions to diagram a .

In diagram c , the exchanged field ϕ can be in the representations $[0, 2, 0]$, $[0, 4, 0]$, $[1, 2, 1]$, $[0, 6, 0]$, $[1, 4, 1]$ and $[2, 2, 2]$. In all cases except the $[0, 2, 0]$ primary discussed above, we have descendent or primary fields in excited Kaluza-Klein multiplets. The quartic couplings $\phi s_2 s_2 s_2$ to the chiral primary of the graviton multiplet then vanish by consistent truncation. Since the integral is finite, all of these contributions vanish.

In diagram d , ϕ can be in any of the representations $[0, 0, 0]$, $[0, 2, 0]$, $[1, 0, 1]$, $[0, 4, 0]$, $[1, 2, 1]$ and $[2, 0, 2]$. Integrals are always convergent. If ϕ comes from a chiral primary in the $[0, \tilde{\delta}, 0]$ with $\tilde{\delta} \geq 3$, the coupling at the lower vertex vanishes because the associated vertex of chiral primaries is forbidden or extremal (or alternatively by consistent truncation). If, on the other hand, $\tilde{\delta} = 2$, ϕ is in the multiplet of the graviton and consistent truncation forbids the upper vertex.

Summarizing, we have seen that the descendent-exchange diagrams only contribute to the $\langle \mathcal{O}_2 \mathcal{O}_2 \mathcal{O}_2 \mathcal{O}_2 \rangle$ factor in the reduced diagram b' . Observe that diagrams b' and c' in Fig. 4 have the same factored structure as graphs b and $b2$ in the SYM calculation (Figs. 1 and 2), whereas diagram a' in Fig. 4 has the same structure as graph a in Fig. 1. Adding all the non-vanishing contributions, which are given by a' , b' and c' , we find

$$\begin{aligned} & \langle \mathcal{O}_4(x) \mathcal{O}_2(x_1) \mathcal{O}_2(x_2) \mathcal{O}_2(x_3) \mathcal{O}_2(x_4) \rangle_{\text{exchange}} \\ &= \frac{4}{N} \langle \mathcal{O}_2(x) \mathcal{O}_2(x_1) \mathcal{O}_2(x_2) \rangle \langle \mathcal{O}_2(x) \mathcal{O}_2(x_3) \mathcal{O}_2(x_4) \rangle \\ &+ \frac{4}{N} \langle \mathcal{O}_2(x) \mathcal{O}_2(x_1) \rangle \langle \mathcal{O}_2(x) \mathcal{O}_2(x_2) \mathcal{O}_2(x_3) \mathcal{O}_2(x_4) \rangle_{\text{AdS}} + \text{perms..} \end{aligned} \quad (2.22)$$

$\langle \mathcal{O}_2(x) \mathcal{O}_2(x_2) \mathcal{O}_2(x_3) \mathcal{O}_2(x_4) \rangle_{\text{AdS}}$ is the full AdS four-point correlator. It includes exchange (diagram b') and contact (diagram c') contributions. This function has been calculated very recently in [10]. We note that the AdS and field theory four-point functions cannot be compared directly since they are renormalized correlators at strong and weak coupling respectively. Nevertheless comparing Eqs. (2.22) and (2.11), we see that the same general space-time structure is found in both the order- g^2 field theory calculation and the exchange diagram contribution to the AdS calculation.

Finally, there is a contact contribution given by diagram e of Fig. 3:

$$\begin{aligned} & \langle \mathcal{O}_4(x) \mathcal{O}_2(x_1) \mathcal{O}_2(x_2) \mathcal{O}_2(x_3) \mathcal{O}_2(x_4) \rangle_e \\ & \sim \mathcal{G}(4, 2, 2, 2, 2) \int \frac{d^5 y}{y_0^5} K_4(x, y) K_2(x_1, y) K_2(x_2, y) K_2(x_3, y) K_2(x_4, y). \end{aligned} \quad (2.23)$$

As shown in the Appendix, this integral is finite. Furthermore it does not have the factored form we have just discussed: it is not a product of a free function times another factor.

Hence the entire AdS calculation of this five-point function does not give the same space-time structure we found at order g^2 unless the coupling $\mathcal{G}(4, 2, 2, 2, 2)$ vanishes. On the other hand this coupling does vanish according to consistent truncation. Therefore if consistent truncation holds, the space-time structure in the full AdS calculation agrees with the field theory results. This, together with the results for extremal and next-to-extremal functions, suggests that the factorization properties of (sub)-extremal correlators may be extrapolated from weak to strong coupling, at least in the large N limit. This is our basic assumption in order to derive the vanishing of certain supergravity couplings.

3 General near-extremal correlators in field theory

In this section we study near-extremal correlation functions in $\mathcal{N} = 4$ SYM to order g^2 and show that all the Feynman graphs contributing to an E_n^m function factor into at least $n - m - 1$ pieces which have only one point in common: the point at which the highest-dimension operator is inserted. In the following, “factor” (or “piece”) should be understood in that sense.

First, we recall the results in [4] and [5], where it was shown that extremal and next-to-extremal n -point (E_n^0 and E_n^1 , respectively) functions are not renormalized to order g^2 . This means that these correlators have a free-field form and, moreover, the overall coefficient does not depend on g . In the extremal case, each of the non-vanishing Feynman graphs is a product of $n - 1$ (free) two-point functions. The point at which the highest-dimension operator is inserted is common to all the two-point functions. In the next-to-extremal case there is in addition a propagator connecting two of the other operators, such that the corresponding graphs are a product of $n - 2$ factors: $n - 3$ (free) two-point functions times one (free) next-to-extremal three-point function.

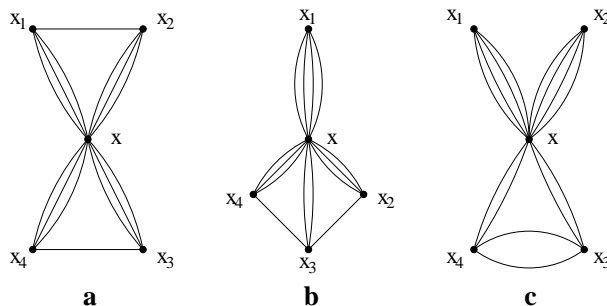


Figure 5: Graphs contributing to E_5^2 functions at the free-field level. Diagram c is disconnected in the particular case $k = 4$, $k_i = 2$ and therefore was not considered in Section 2.1.

Next we consider a general E_5^2 function, $\langle \mathcal{O}_k(x) \mathcal{O}_{k_1}(x_1) \mathcal{O}_{k_2}(x_2) \mathcal{O}_{k_3}(x_3) \mathcal{O}_{k_4}(x_4) \rangle$ with $k =$

$k_1 + k_2 + k_3 + k_4 = 4$. The Feynman graphs contributing at the free-field level are shown in Fig. 5.

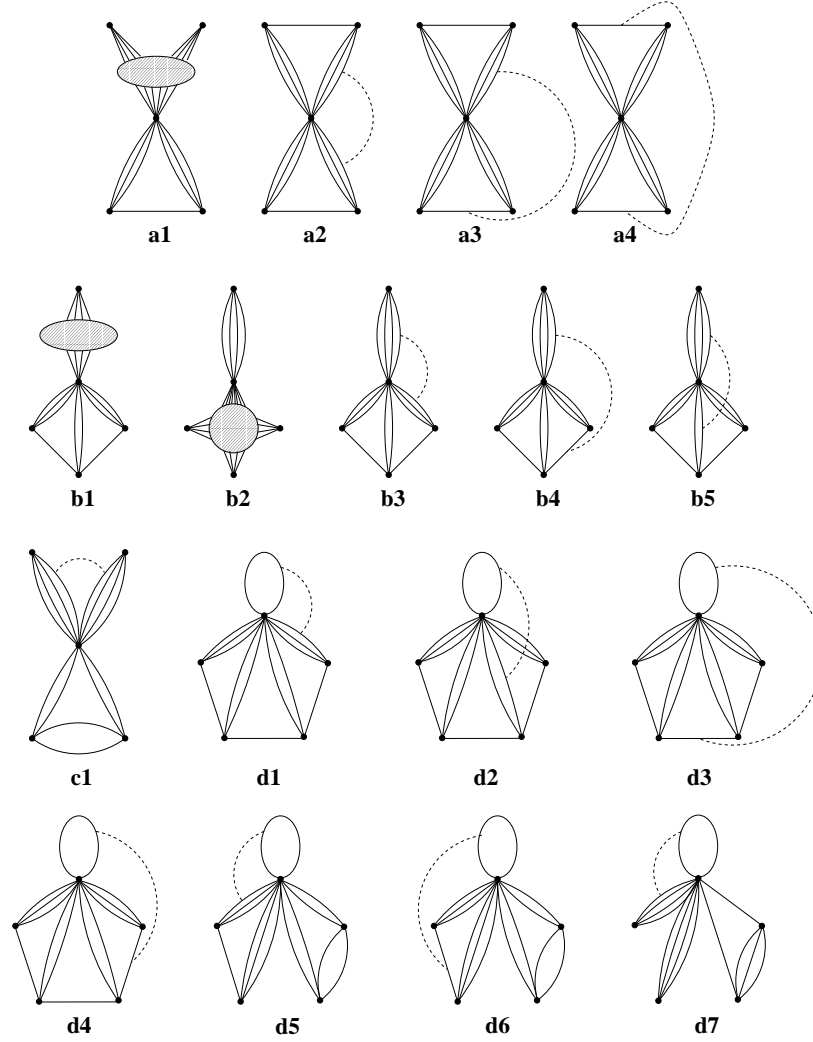


Figure 6: Feynman graphs contributing to an E_5^2 function at order g^2 .

The Feynman graphs that contribute at order g^2 are depicted in Fig. 6. The graphs $a1 - c1$ are radiative corrections of the graphs in Fig. 5. Graphs with two “tadpoles” connected by a dashed line vanish trivially due to the symmetry in the colour indices in the highest-dimension operator, and we do not display them explicitly here or in the subsequent. Graphs $a1$ and $b1$ vanish due to non-renormalization theorems for two-point and three-point correlators [17]. Indeed, as was discussed in [5], the operator $\mathcal{O}_{k'}(x)$ entering the relevant two-point and three-point functions is in the $[0, k', 0]$ representation of the $SU(4)$ flavour group and the extra colour-group generators appearing in the trace of this operator do not spoil the validity of the non-renormalization proofs in [17]. As in Section 2, all the

remaining graphs except $b2$ vanish due to the symmetries in the colour indices. We show this explicitly for graph $b4$.

In order to simplify the equations we introduce the following schematic notation:

$$\{b_1 b_2 \cdots b_s\} = \text{Str}(T^{b_1} T^{b_2} \cdots T^{b_s} T^{a_i} \cdots T^{a_{i+r-1}}), \quad (3.1)$$

where a_i, \dots, a_{i+r-1} are the colour indices of the r legs of a given operator which are attached to the highest-dimension operator, $\mathcal{O}_k(x)$, and b_1, \dots, b_s are extra colour indices. Moreover we write the trace of the operator $\mathcal{O}_k(x)$ as

$$\{a\} = \text{Str}(T^{a_1} \cdots T^{a_k}), \quad (3.2)$$

and a trace with a commutator as, e.g.,

$$\{[b, c]\} = \text{Str}([T^b, T^c] T^{a_i} \cdots T^{a_{i+r-1}}), \quad (3.3)$$

where the trace on the *r.h.s.* is not symmetrized under $b \leftrightarrow c$. With this notation, the contribution of graph $b4$ reads

$$\begin{aligned} b4 &\sim \left(A f^{a_1 b p} f^{c d p} + B f^{a_1 c p} f^{b d p} + C f^{a_1 d p} f^{b c p} \right) \\ &\quad \cdot \text{Str}(T^{a_1} \cdots T^{a_k}) \text{Str}(T^b T^{a_2} \cdots T^{a_{k_1}}) \text{Str}(T^d T^{a_{k_1+1}} \cdots T^{a_{k_1+k_2-1}}) \\ &\quad \cdot \text{Str}(T^c T^e T^{a_{k_1+k_2}} \cdots T^{a_{k_1+k_2+k_3-3}}) \text{Str}(T^e T^{a_{k_1+k_2+k_3-2}} \cdots T^{a_{k_1+k_2+k_3+k_4-4}}) \\ &\equiv \left(A f^{a_1 b p} f^{c d p} + B f^{a_1 c p} f^{b d p} + C f^{a_1 d p} f^{b c p} \right) \\ &\quad \cdot \{a\} \{b\} \{d\} \{c e\} \{e\}, \end{aligned} \quad (3.4)$$

where A, B and C are functions of space-time and flavour. We show in turn that the three terms vanish, using the identities $[T^a, T^c] = i f^{a c p} T^p$ and

$$\sum_{i=1}^r \text{Tr}(M_1 \cdots [M_i, N] \cdots M_r) = 0, \quad (3.5)$$

where M_i, N is any set of matrices. The same identity holds for the symmetric trace.

For the term with coefficient A , contracting one of the structure constants with a group constant inside a trace, we find

$$\begin{aligned} A\text{-term} &\sim \{a\} \{[a_1, p]\} \{d\} \{c e\} \{e\} \\ &\sim \{a\} \sum_i \{p[a_1, a_i]\} \{d\} \{c e\} \{e\} \\ &= 0, \end{aligned} \quad (3.6)$$

where in the last identity we have used the fact that in each term there is a contraction of an antisymmetric commutator, $[T^{a_1}, T^{a_i}]$, times a symmetric trace, $\{a\}$. Similarly, for the

term with coefficient B we have

$$\begin{aligned}
B\text{-term} &\sim \{a\}\{b\}\{d\}\{[a_1, p]e\}\{e\} \\
&\sim \{a\}\{b\}\{d\}(\{p[a_1, e]\} + \sum_i \{pe[a_1, a_i]\})\{e\} \\
&\sim \{a\}\{b\}\{d\}\{pq\}f^{a_1eq}\{e\} \\
&\sim \{a\}\{b\}\{d\}\{pq\}\{[a_1, q]\} \\
&\sim \{a\}\{b\}\{d\}\{pq\} \sum_i \{q[a_1, a_i]\} \\
&= 0.
\end{aligned} \tag{3.7}$$

Finally, let us show that the term with coefficient C vanishes as well:

$$\begin{aligned}
C\text{-term} &\sim \{a\}\{b\}\{[a_1, p]\}\{ce\}\{e\} \\
&\sim \{a\}\{b\} \sum_i \{p[a_1, a_i]\} \\
&= 0.
\end{aligned} \tag{3.8}$$

Hence graph $b4$ vanishes. The essential step in the proof is to use the identity (3.5) to shift antisymmetric combinations of indices arising from the structure constants between traces, until a commutator $[T^{a_i}, T^{a_j}]$ is obtained, which vanishes when contracted with $\{a\}$. One can prove in a similar manner that graphs $a2 - a4$, $b3$, $b5$, $c1$, and $d1 - d7$ vanish as well. On the other hand, there are graphs of the general form $b2$ that give finite contributions because they cannot be reduced to a sum of terms containing a commutator $[T^{a_i}, T^{a_j}]$. Nevertheless we see that $b2$ has the factored form

$$\begin{aligned}
&\langle \mathcal{O}_k(x)\mathcal{O}_{k_1}(x_1)\mathcal{O}_{k_2}(x_2)\mathcal{O}_{k_3}(x_3)\mathcal{O}_{k_4}(x_4) \rangle_{b2} \\
&= \frac{1}{N} \sqrt{k k_1 (k - k_1)} \langle \mathcal{O}_{k_1}(x)\mathcal{O}_{k_1}(x_1) \rangle \langle \mathcal{O}_{k-k_1}(x)\mathcal{O}_{k_2}(x_2)\mathcal{O}_{k_3}(x_3)\mathcal{O}_{k_4}(x_4) \rangle^{(1)}, \tag{3.9}
\end{aligned}$$

which is a product of a free two-point function and an E_4^2 four-point function. In this equation it is understood that the colour generators of the operators $\mathcal{O}_{k_1}(x)$ and $\mathcal{O}_{k-k_1}(x)$ are included inside the same trace, such that the two factors are coupled by colour. However, the colour indices within the first factor are contracted and eventually a product of two functions which are colour singlets is obtained. Therefore all the graphs factor into at least two pieces and the E_5^2 function has, to order g^2 , the form

$$\begin{aligned}
\langle \mathcal{O}_k(x)\mathcal{O}_{k_1}(x_1)\mathcal{O}_{k_2}(x_2)\mathcal{O}_{k_3}(x_3)\mathcal{O}_{k_4}(x_4) \rangle &= \frac{1}{N} \sqrt{k(k_1 + k_2 - 2)(k_3 + k_4 - 2)} \\
&\cdot \langle \mathcal{O}_{k_1+k_2-2}(x)\mathcal{O}_{k_1}(x_1)\mathcal{O}_{k_2}(x_2) \rangle \langle \mathcal{O}_{k_3+k_4-2}(x)\mathcal{O}_{k_3}(x_3)\mathcal{O}_{k_4}(x_4) \rangle \\
&+ \frac{1}{N} \sqrt{k k_1 k_2 (k_3 + k_4 - 4)} \langle \mathcal{O}_{k_1}(x)\mathcal{O}_{k_1}(x_1) \rangle \langle \mathcal{O}_{k_2}(x)\mathcal{O}_{k_2}(x_2) \rangle \langle \mathcal{O}_{k_3+k_4-4}(x)\mathcal{O}_{k_3}(x_3)\mathcal{O}_{k_4}(x_4) \rangle \\
&+ \frac{1}{N} \sqrt{k k_1 (k - k_1)} \langle \mathcal{O}_{k_1}(x)\mathcal{O}_{k_1}(x_1) \rangle \langle \mathcal{O}_{k-k_1}(x)\mathcal{O}_{k_2}(x_2)\mathcal{O}_{k_3}(x_3)\mathcal{O}_{k_4}(x_4) \rangle' + \text{perms.}, \tag{3.10}
\end{aligned}$$

where

$$\langle \mathcal{O}_{k_1+k_2-2p}(x)\mathcal{O}_{k_1}(x_1)\mathcal{O}_{k_2}(x_2) \rangle = \frac{1}{N} \frac{\sqrt{(k_1+k_2-2p)k_1k_2}}{(x-x_1)^{2(k_1-p)}(x-x_2)^{2(k_2-p)}(x_1-x_2)^{2p}}, \quad (3.11)$$

and the square roots account for the large N Wick factors and the normalization. The prime in the four point function in (3.10) indicates that a factorized free-field contribution to this four point function has been explicitly written in the second term of the equation and must not be included again. Observe that the sum of the degrees of extremality of the factors in each term is 2 (*i.e.*, next-to-next-to-extremal). Schematically Eq. (3.10) can be written

$$E_5^2 = E_3^1 E_3^1 + E_2^0 E_2^0 E_3^2 + E_2^0 E_4^2. \quad (3.12)$$

The extension of this detailed analysis to E_n^m functions for $n > 5$ and $m \geq 2$ is very tedious, and we limit the discussion to the demonstration of factorization properties through order g^2 . Specifically we will argue that

- E_6^2 functions split into at least three factors:

$$E_6^2 = E_2^0 E_3^1 E_3^1 + E_2^0 E_2^0 E_4^2. \quad (3.13)$$

- E_6^3 functions split into at least two factors:

$$E_6^3 = E_2^0 E_5^3 + E_3^1 E_4^2 + E_3^2 E_4^2 + E_3^3 E_4^0. \quad (3.14)$$

- In the general case E_n^m splits into at least $n - m - 1$ factors:

$$E_n^m = \sum_{\{n_j, m_j\}} \prod_{i=1}^{n-m-1} E_{n_i}^{m_i}, \quad (3.15)$$

where $\sum_{i=1}^{n-m-1} n_i = 2(n-1) - m$ and $\sum_{i=1}^{n-m-1} m_i = m$. If $m \leq n - 3$ each term factors into at least two pieces and the maximum value of n_i is $n - 1$.

The qualification “at least” is meant to indicate that there are graphs in which more factors occur. For instance, in graph *c* of Fig. 7 below, the factor E_4^2 of the last term in (3.13) splits in turn into $E_2^0 E_3^2$. Even with this limited aim, the discussion is complicated and some readers may wish to proceed to Section 4.

Let us consider six-point functions $\langle \mathcal{O}_k(x)\mathcal{O}_{k_1}(x_1)\cdots\mathcal{O}_{k_5}(x_5) \rangle$. The E_6^2 correlators have $k = \sum_{i=1}^5 k_i - 4$. The free-field Feynman graphs for such a function are displayed in Figure 7. We include graphs with tadpoles, which vanish at this order (because the primary operators are traceless tensors in flavour space) but can be used to construct order g^2 graphs. The graphs in Figure 7 are similar to the ones contributing to the E_5^2 functions studied above,

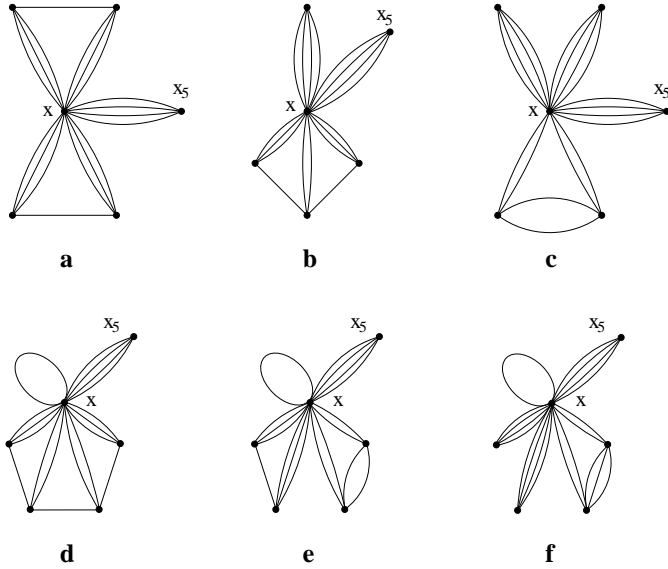


Figure 7: Feynman graphs contributing to an E_6^2 function at the free-field level.

but with an additional “rainbow” of propagators connecting the highest-dimension operator to the additional operator (at x_5 in the figures). The order g^2 corrections can be classified in three groups: graphs that factor into the E_5^2 -graphs times a free two-point subgraph involving the new operator, corrections inside the rainbow and graphs that connect the new rainbow to the rest of the free-field graph. Using the results above it is clear that the graphs of the first group have at least three factors, two of which are free-field functions. The corrections within the rainbow are corrections to a two-point function and vanish. Finally, with the method used above for graph $b4$ of Fig. 6, the graphs of the third kind can be shown to either vanish or factor into three factors, two of which are free-field functions. The second possibility occurs only when the new rainbow is connected to one of the two lines at the bottom of graph c . Summarizing, all graphs have at least three factors and we find the structure in (3.13).

The Feynman graphs that contribute at the free-field level to an E_6^3 function ($k = \sum_{i=1}^5 k_i - 6$) are depicted in Figure 8. It is useful to introduce the following definition: We denote as “T graphs” those graphs which have no closed loops after removing all the lines connected to the highest-dimension operator. A T_k graph is defined to be a T graph with k factors. We can then distinguish four kinds of graphs in Figure 8:

1. Graphs with $q \geq 3$ factors: d , e , f and g .
2. Graphs with one tadpole and at least two factors: i .
3. T_2 graphs: a , b and c .

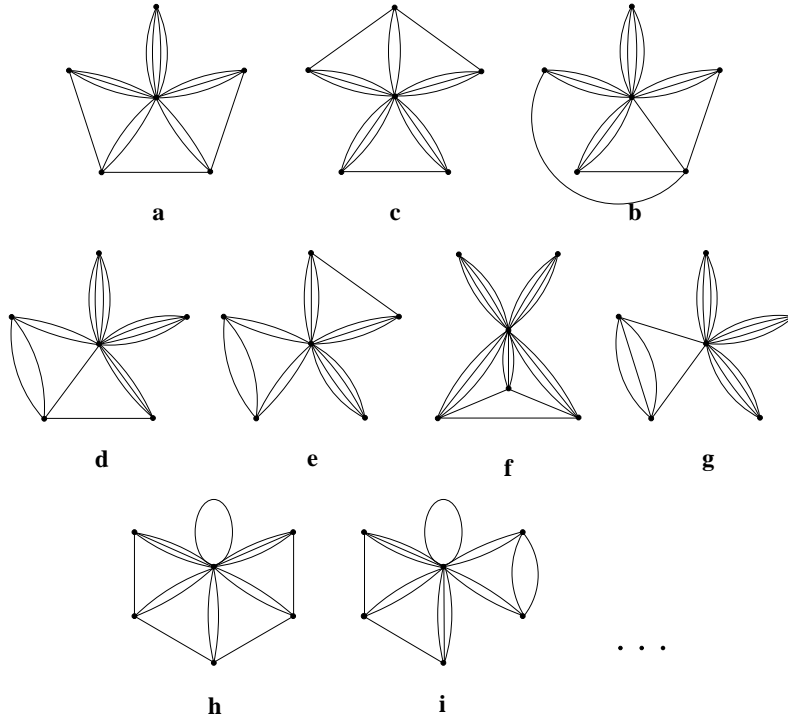


Figure 8: Feynman graphs contributing to an E_6^3 function at the free-field level. The dots stand for other graphs with one tadpole and two or more pieces.

4. T_1 graphs with one tadpole: h .

Let us consider now the order g^2 graphs, that are either self-energy corrections or can be constructed inserting a dashed line in the graphs of Figure 8. Self-energy corrections do not change the number of factors of the graph and we do not need to study them, although we observe that they cancel other corrections in such a way that two- and three-point factors are not renormalized. From now on, we consider only dashed-line graphs. Order g^2 graphs constructed by inserting a dashed line into the free-field graphs of the first kind obviously have at least two factors, as a single line cannot connect three or more pieces. The same applies to order g^2 graphs constructed from graphs of the second kind since one end of the dashed line has to be connected to the tadpole line. Finally, we prove below for any number of points that T graphs do not have order g^2 corrections connecting the different factors or one factor to a tadpole. This means that order g^2 graphs constructed from graphs of the third kind factor into two pieces and that the order g^2 graphs constructed from graphs of the fourth kind vanish. Therefore we conclude that to order g^2 all non-vanishing graphs factor into at least two pieces.

Furthermore each graph has a global degree of extremality equal to 3, *i.e.*, it is a product $\prod_{i=1}^p E_{n_i}^{m_i}$ with $\sum_{i=1}^p n_i = 6 + p - 1$ and $\sum_{i=1}^p m_i = 3$. This property can be read directly

from the graphs in Figure 8. Therefore we obtain the structure written in (3.14).

The analysis of the six-point correlators can be easily generalized to E_n^m functions, $\langle \mathcal{O}_k(x) \mathcal{O}_{k_1}(x_1) \cdots \mathcal{O}_{k_{n-1}}(x_{n-1}) \rangle$ with $k = \sum_{i=1}^{n-1} k_i - 2m$. It turns out that to order g^2 an E_n^m function, $m \leq n - 2$, is a sum of terms that factor into at least $n - m - 1$ pieces. The essential ingredient in the proof is the fact that the Feynman graphs contributing to an E_n^m function at the free-field level fall among the following classes:

1. Graphs with $q \geq n - m$ factors.
2. Graphs with one tadpole and at least $n - m - 1$ factors.
3. T_{n-m-1} graphs.
4. T_{n-m-2} graphs with one tadpole.

To see this, consider first graphs without tadpoles. These graphs have m lines that are not connected to x . Let us add these m lines in turn. After adding one line we are left with a graph with $n - 2$ factors. Then we add another line. If it connects the same two operators that were joined by the first line, we obtain a non-T graph with $n - 2$ factors. On the other hand, if one end of the second line is attached to an operator that were not connected to the first line, we get a T graph with $n - 3$ factors. The third line can either connect different factors or connect operators within one factor. In the first case, one gets a non-T graph with $n - 3$ factors or a T graph with $n - 4$ factors, depending on the choice of the second line. In the second case one gets a non-T graph with $n - 2$ or $n - 3$ factors. We can proceed recursively and find that after adding the m th line we get a T graph with $n - m - 1$ factors or a non-T graph with $q \geq n - m$ factors. If the graph has one tadpole there are $m + 1$ lines that are not connected to x , and the argument can be repeated with $m \rightarrow m + 1$.

The proof that the order g^2 graphs constructed from these ones factor into $n - m - 1$ graphs is identical to the proof given above for $n = 6$. The only non-trivial ingredient is that order g^2 graphs constructed from free-field T_q graphs factor into q parts or vanish. We show this next.

First, we observe that the following property holds:

$$f^{bcp}\{cd_1 \cdots d_k\} \sim \sum_{i=1}^{r-1} f^{ba_iq}\{pd_1 \cdots d_k\} + \sum_{i=1}^k f^{bd_iq}\{pd_1 \cdots \widehat{d}_i \cdots d_k\}, \quad (3.16)$$

where r is the number of lines of the given operator connected to the highest dimension operator. We see that all the terms on the *r.h.s.* have an f with one of the indices of the f on the *l.h.s.*, and one of the indices in the trace at the *l.h.s.*. In other words: p changes, b is replaced by a_i or d_i and c stays the same.

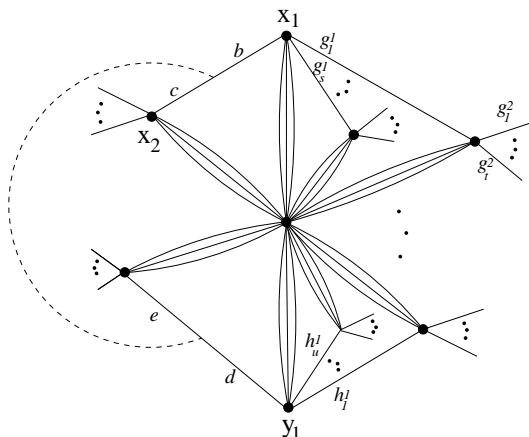


Figure 9: Relevant part of a general order- g^2 correction to a T graph.

Consider now a general T_p graph with $p \geq 2$ and one dashed line connecting the “external” (*i.e.*, not connected to the highest-dimension operator) lines of two different factors. In Fig. 9 we show a part of this graph. There are three contributions:

1. $f^{bcp} f^{dep}$. The index b appears in the trace of the operator at x_1 . Using the relation (3.16) we obtain a sum of terms that contain $f^{a_i^1 c q^1}$ or $f^{g_i^1 c q^1}$. This last f is in turn contracted with an index in another trace and we can apply the same relation to obtain terms with $f^{a_i^2 c q^2}$ or with $f^{g_i^2 c q^2}$. We repeat the procedure for the terms that do not contain an f with an a_i until we reach an operator with only one external leg. Then all terms contain $f^{a_i c q}$. Since c appears in the trace of the operator at x_2 , we can use the same method but keeping now a_i fixed. Finally the expression is reduced to a series of terms that contain $f^{a_i a_j q}$, which is antisymmetric under $a_i \leftrightarrow a_j$. Since all the terms also contain the symmetric trace $\{a\}$, they vanish.
2. $f^{bdp} f^{cep}$. The indices in the first f can be shifted just as above until a sum of terms containing $f^{a_i d q}$ is obtained. This f is contracted to the trace in y_1 through the index d , and can be transformed into a sum of terms with either $f^{a_i a_j^1 q^1}$ or $f^{a_i h_j^1 q^1}$. The first kind of terms vanish when contracted with $\{a\}$ and the second kind can be transform until all terms contain $f^{a_i a_j q^1}$. All these terms vanish when contracted with $\{a\}$.
3. $f^{bep} f^{cdp}$. The previous argument can be applied to this case as well.

The same can be argued if one or both ends of the dashed line were connected to a rainbow or to a tadpole. Note that it is essential for the argument that, when the indices in one f are shifted by using Eq. (3.16), the two new indices are different from all the indices in previous steps. This would not occur if there were loops of external lines. For this reason the proof only applies to T graphs. Since the different factors of a T graph cannot be connected at order g^2 we conclude that their factored structure is preserve to this order.

Moreover, the sum of the degrees of extremality of the factors of any term in an E_n^m function is equal to m . Indeed, if a Feynman graph factors into two or more functions it can be written as $E_{n_1}^{m_1} E_{n_2}^{m_2}$, with $n_1 + n_2 = n + 1$. In general, each factor can be further factored. Both factors have x as a common point. From the degrees of extremality of the two factors it follows that $\sum_{i=1}^{n_1-1} k_i - 2m_1$ legs of the operator $\mathcal{O}_k(x)$ enter the first factor and $\sum_{i=1}^{n_2-1} k_i - 2m_2$ legs of this operator enter the second factor. Since the operator $\mathcal{O}_k(x)$ has k legs,

$$\begin{aligned} k &= \sum_{i=1}^{n_1-1} k_i - 2m_1 + \sum_{i=1}^{n_2-1} k_i - 2m_2 \\ &= \sum_{i=1}^{n-1} k_i - 2(m_1 + m_2), \end{aligned} \tag{3.17}$$

and from the m -extremality condition, $m = m_1 + m_2$. The same procedure can be applied to the subfactors of $E_{n_1}^{m_1}$ and $E_{n_2}^{m_2}$. An alternative way of understanding this property is noting that the degree of extremality of each factor is given by the number of lines in that factor that are not connected to x . This proves the structure written in (3.15).

4 General near-extremal correlators in AdS

The $AdS_5 \times S^5$ supergravity cubic and quartic couplings of chiral primary fields have been calculated in [15] and [31], respectively. In the extremal case, *i.e.*, when the conformal dimension of one field equals the sum of the remaining conformal dimensions, these couplings vanish. Furthermore the requirement that the AdS amplitudes have to be finite for non-coincident points implies that the couplings of extremal n -field vertices must vanish for any $n \geq 3$ [29]. As we show in the Appendix, there are boundary contributions and the Witten diagrams of extremal n -point functions reduce to a product of two-point functions connected to the point x at which the highest-dimension operator is inserted. This is illustrated in Fig. 10. The space-time structure of these diagrams agree with the free-field approximation. Furthermore, in [29, 30] it was shown that the coefficient multiplying this structure is not renormalized.

In [5] it was shown that the next-to-extremal couplings of n chiral primaries have to vanish, since otherwise the AdS and the field-theoretical calculations of E_n^1 functions would not agree. This has been recently checked explicitly for $n = 4$ [6]. All non-vanishing Witten diagrams contributing to the E_n^1 functions then reduce to products of $n - 3$ two-point functions times one next-to-extremal three-point function, all of them with x as a common point, as we show in Fig. 10. The space-time structure of the reduced diagrams agrees with the field-theoretical calculation [5]. For E_4^1 functions we have also checked that the coefficient of the AdS structure agrees with the result found in field theory. The calculation is similar to the ones we show in the Appendix below.

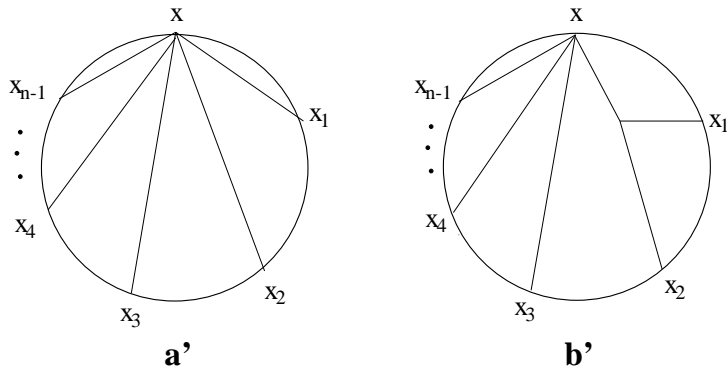


Figure 10: Non-vanishing contributions to E_n^0 (diagram a') and E_n^1 (diagram b') functions.

This analysis can be extended to other E_n^m functions. It can be shown in general that, as long as certain supergravity couplings vanish, the AdS calculation gives the same space-time structure as the order g^2 calculation, up to the detailed form of the factors that are renormalized. We have already shown this for the simplest E_n^2 function in Section 2.2.

The calculation of a general E_5^2 function $\langle \mathcal{O}_k \mathcal{O}_{k_1} \mathcal{O}_{k_2} \mathcal{O}_{k_3} \mathcal{O}_{k_4} \rangle$ in AdS is very similar to the one for $\langle \mathcal{O}_4 \mathcal{O}_2 \mathcal{O}_2 \mathcal{O}_2 \mathcal{O}_2 \rangle$ and we discuss only the new features:

1. We have checked for general k_i 's that the coefficient of diagram a in Fig. 3 agrees with the coefficient of the field-theory graph a in Fig. 5 as given by the first term in (3.10). This calculation may be found in the Appendix below Eq. (A.14).

2. Diagram d of Fig. 3 does not vanish in general, but gives a new reduced diagram, d' in Fig. 4 (the same structure results from diagram b' when the upper vertex is extremal). This reduced diagram has the same form as graph c in Fig. 5, which gives the second term in the field theory result (3.10). It is interesting to note that this structure appears neither in field theory nor in AdS for the connected $\langle \mathcal{O}_4 \mathcal{O}_2 \mathcal{O}_2 \mathcal{O}_2 \mathcal{O}_2 \rangle$. It is possible to calculate the coefficient of diagram d' as well, but this requires considerable processing of the results for quartic couplings in [33].

3. The discussion of descendent exchange becomes more complicated. For diagrams in which quartic couplings appear, consistent Kaluza-Klein truncation is not sufficient for general k_i , but it motivates the assumption³ that a coupling with descendents vanishes whenever the associated coupling of chiral primaries does. With this assumption, one can easily extend the analysis of descendents in Section 2.2 and conclude that they only contribute to four-point factors.

4. The contact diagram spoils the factorization property. Hence the result in supergravity

³For scalar and vector descendents there is evidence from AdS diagrams and field theory to support this assumption. We do not discuss it here.

only agrees with the factorization we have found at weak coupling if the E_5^2 couplings vanish. This is an extension of consistent Kaluza-Klein truncation.

More general functions will be considered in the next section. There we reverse the argument and derive the vanishing of certain supergravity couplings from the requirement that the field-theoretical calculation to order g^2 and the AdS calculation give the same factored structure.

5 Vanishing near-extremal supergravity couplings

In this section we show that E_n^m supergravity couplings vanish for any $m \leq n - 3$ if the following assumptions hold:

1. Witten diagrams are finite for non-coincident external points.
2. The factorization of E_n^m functions, $m \leq n - 3$ that we have found (for any N) to order g^2 is preserved at large t'Hooft coupling in the large N limit.
3. A vertex with one or more descendents has a vanishing coupling if the coupling of the associated chiral primary vertex vanishes.

We do not use known results about supergravity couplings in the argument. The fact that extremal cubic and quartic couplings and next-to-extremal quartic couplings do vanish then supports the validity of the assumptions above.

We also need the results of the Appendix, which are summarized by

- The integral over y in a Witten diagram is divergent if and only if the vertex at y is extremal and the highest-dimension field entering that vertex propagates into the boundary (at point x).
- If this is the case, the divergence is logarithmic and comes from the region $y \sim x$.

In analytic continuation this divergence appears as a pole that, according to the first assumption, must be cancelled by a zero coming from the coupling. When the regulator is removed, the diagram factors into at least two pieces.

The proof proceeds by induction in the number of points, n . The induction starts for $n = 3$, $m = 0$. We consider an extremal three-point function. The integral is divergent and, according to the first assumption, the coupling must vanish. Therefore, the E_3^m couplings vanish for any $m \leq 3 - 3 = 0$. Furthermore, the diagram factors into two two-point functions, in agreement with the field-theoretical results.

Let now $n \geq 3$. Suppose that the E_p^m couplings vanish for all $m \leq p - 3$, $p \leq n$. We have to show that the E_{n+1}^m couplings vanish for $m \leq 2$.

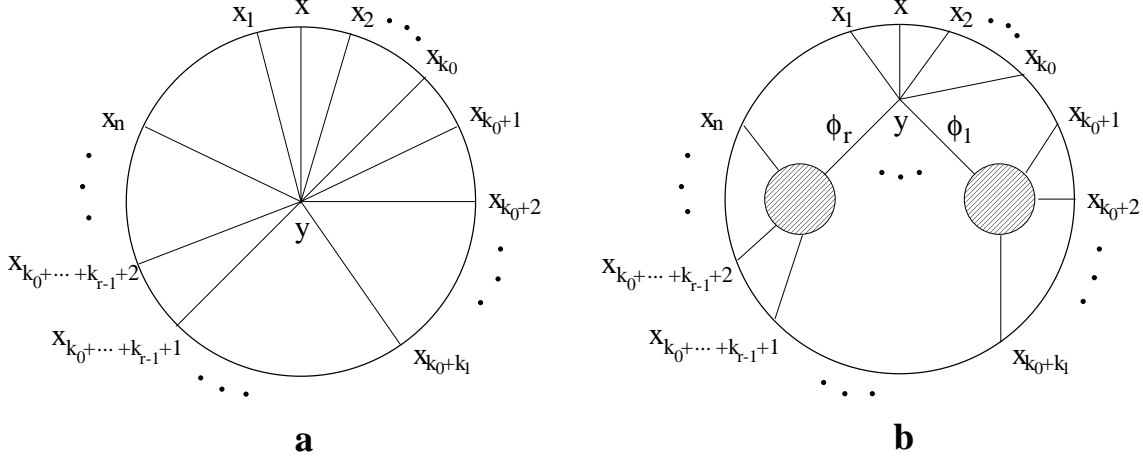


Figure 11: Witten diagrams contributing to an E_{n+1}^m function.

Consider an E_{n+1}^m function $\langle \mathcal{O}_\Delta(x) \mathcal{O}_{\Delta_1}(x_1) \cdots \mathcal{O}_{\Delta_n} \rangle$, with $m \leq n - 2$. This means that $\Delta = \sum_{i=1}^n \Delta_i - 2m$. Δ and Δ_i are the conformal dimensions of the chiral primary operators, which coincide with the non-vanishing Dynkin labels of their $SU(4)$ representation. Two kinds of diagrams contribute: contact and exchange. All the exchange diagrams are of the general form shown in Fig. 11, with $1 \leq k_0 \leq n - 2$. We consider first diagrams that involve only primary exchanges. The exchanged fields ϕ_1, \dots, ϕ_r are in the representations $[0, \delta_1, 0], \dots, [0, \delta_r, 0]$, and have dimensions $\delta_1, \dots, \delta_r$, respectively. Only the sets of fields with

$$\sum_{j=1}^r \delta_j = \sum_{i=k_0+1}^n \Delta_i - 2m, \quad \sum_{i=k_0+1}^n \Delta_i - (2m - 1), \dots, \sum_{i=k_0+1}^n \Delta_i. \quad (5.1)$$

are allowed by $SU(4)_R$. We distinguish three possibilities:

1. $\sum_{j=1}^r \delta_j = \sum_{i=k_0+1}^n \Delta_i - 2m.$
2. $\sum_{i=k_0+1}^n \Delta_i - 2(m - 1) \leq \sum_{j=1}^r \delta_j \leq \sum_{i=k_0+1}^n \Delta_i - 2(m - k - r + 2).$
3. $\sum_{j=1}^r \delta_j \geq \sum_{i=k_0+1}^n \Delta_i - 2(m - k_0 - r + 1).$

We study the three cases in turn.

Case (1): Since $\sum_{i=k_0+1}^n \Delta_i - 2m = \Delta - \sum_{i=1}^{k_0} \Delta_i$, the vertex at y is extremal and vanishes due to the induction hypothesis. On the other hand, the integral diverges since the field with highest dimension, Δ , propagates to the boundary. Hence the diagram factors into $(E_2^0)^{k_0} E_{n-k_0+1}^m$, as shown in Fig. 12.

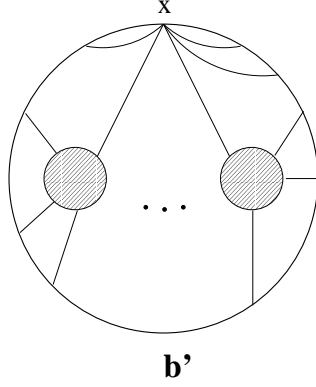


Figure 12: Non-vanishing contribution to an E_{n+1}^m function.

Case (2): Since $\sum_{i=k_0+1}^n \Delta_i - 2(m - k - r + 2) = \Delta - \sum_{i=1}^{k_0} \Delta_i + 2(k - 1)$, the vertex at y is $E_{k_0+2}^p$ with $p \leq (k + 2) - 3$ and is zero by the induction assumption. Because the integral over y is convergent and the other possible divergences are cancelled by zeros in the extremal couplings, the diagram vanishes (see the Appendix).

Case (3) We have the inequality

$$\sum_{i=k_0+1}^n \Delta_i - 2(m - k_0 - r + 1) \geq \sum_{j=1}^r \left[\sum_{i=k_0+\dots+k_{j+1}}^{k_0+\dots+k_{j+1}} \Delta_i - 2(k_j - 1) \right] + 2. \quad (5.2)$$

If $\delta_1 \geq \sum_{i=k_0+1}^{k_0+k_1} - 2(k_1 - 2)$, the subdiagram involving the points y and $x_{k_0+1}, \dots, x_{k_0+k_1}$ and the points in the corresponding blob is an $E_{k_1+1}^p$ diagram with $p \leq (k_1 + 1) - 3$ and the highest-dimension field (ϕ_1) propagating into the bulk, which we denote as $\tilde{E}_{k_1+1}^p$. If, on the contrary, $\delta_1 \leq \sum_{i=k_0+1}^{k_0+k_1} - 2(k_1 - 1)$, the following relation holds:

$$\sum_{j=2}^r \delta_j \geq \sum_{j=2}^r \left[\sum_{i=k_0+\dots+k_{j+1}}^{k_0+\dots+k_{j+1}} \Delta_i - 2(k_j - 1) \right] + 2. \quad (5.3)$$

If $\delta_2 \geq \sum_{i=k_0+k_1+1}^{k_0+k_1+k_2} - 2(k_2 - 2)$, the corresponding subdiagram is an $\tilde{E}_{k_2+1}^p$ function with $p \leq (k_2 + 1) - 3$. Otherwise, we have a relation similar to the one above involving $\sum_{j=3}^r \delta_j$. Iteratively, if $\delta_j \leq \sum_{i=k_0+\dots+k_{j-1}+1}^{k_0+\dots+k_j} - 2(k_j - 1)$ for $j = 1, \dots, r - 1$, we find that

$$\delta_r \geq \sum_{i=k_0+\dots+k_{r-1}+1}^{k_0+\dots+k_r} \Delta_i - 2(k_r - 2), \quad (5.4)$$

such that the corresponding subdiagram is an $\tilde{E}_{k_r+1}^p$ function with $p \leq (k_r + 1) - 3$. Hence, at least one of the subdiagrams connected to y is an $\tilde{E}_{k_j+1}^p$ function with $p \leq (k_j + 1) - 3$. The analysis of the entire diagram b can be applied to this subdiagram to show that it

vanishes. We have again three possibilities. The only difference is that in the equivalent of case (1) the integral is finite because the highest-dimension field (ϕ) propagates into the bulk. More details are given in the Appendix. The iteration ends when all the subdiagrams are contact diagrams, which vanish because the induction hypothesis implies that the $E_{k_j+1}^p$ coupling is zero for $p \leq (k_j + 1) - 3$.

Therefore, the cases (2) and (3) lead to vanishing diagrams, whereas the case (1) gives a reduced diagram with at least two factors. Consider now the case when at least one of the fields ϕ_j is a descendent. Then, if Δ_{ϕ_j} denotes the conformal dimension of each field, $\sum_{j=1}^r \Delta_{\phi_j} > \sum_{i=k_0+1}^n \Delta_i - 2m$ and the vertex at y is sub-extremal. Hence the integral over y is finite. On the other hand, if ϕ_j is a descendent, it descends from a chiral primary field in a representation $[0, \tilde{\delta}_j, 0]$ with $\tilde{\delta}_j > (\delta_j)_{\min}$, where $(\delta_j)_{\min}$ is the minimal dimension allowed by $SU(4)$ if ϕ_j were chiral primary. All the possibilities can be discussed just as in the pure chiral primary case, but changing some δ_j by $\tilde{\delta}_j$. Using assumption 3, we conclude that in all cases one or more of the couplings involved in the diagram vanish if the induction hypothesis holds.

We have shown that all the exchange diagrams either vanish or factor into at least two pieces. Finally, there is a contact diagram contributing to the E_{n+1}^m function (diagram a in Fig. 11). In the extremal case, $m = 0$, this diagram has a logarithmic divergence that has to be cancelled by a zero in the coupling. Hence the E_{n+1}^0 coupling vanishes. If $m \geq 1$ the diagram is finite and does not have a factored structure. Since the non-vanishing exchange diagrams factor, the non-factored contribution of the contact diagram survives in the full function. On the other hand, we have shown in Section 3 that, to order g^2 , E_{n+1}^m functions factor into at least two pieces if $m \leq n - 3$. According to the second assumption (and the Maldacena conjecture), the AdS calculation should also give a factored structure. Therefore, the E_{n+1}^m couplings must vanish in order for the contact diagram not to contribute. This completes the induction.

Finally, we observe that the first assumption can be relaxed: It is sufficient to require that the sum of the Witten diagrams contributing to an AdS amplitude is finite. This however, complicates the description of the proof and for that reason we have chosen here an slightly stronger assumption.

6 Conclusions

The main results of this paper are

1. Through order g^2 , field theory graphs for near-extremal n -point functions have a factored structure.
2. This structure is shown to be matched exactly by exchange diagrams in AdS super-

gravity for the five-point function $\langle \mathcal{O}_4 \mathcal{O}_2 \mathcal{O}_2 \mathcal{O}_2 \mathcal{O}_2 \rangle$. For more general E_5^2 functions an additional technical assumption about descendent couplings is required to reach the same conclusion.

3. For E_5^2 functions we show that there are unique supergravity diagrams which match the corresponding field theory graphs in form and coefficient.
4. For E_n^m functions with $n > 5$ and $m \leq n - 3$ we establish a similar but less precise correspondence between field theory and supergravity.
5. The correspondence would be spoiled by non-factored supergravity contact diagrams unless the associated near-extremal couplings vanish. We therefore conjecture that E_n^m couplings do vanish when $m \leq n - 3$. For some cases this is a consequence of consistent Kaluza-Klein truncation and it is a natural extension of known results for $n = 3, 4$. It remains to explain the pattern of vanishing couplings, which is presumably a consequence of the reduction of Type II B supergravity on the internal space S^5 .

Acknowledgements

We thank Leonardo Rastelli for useful discussions. The research of E.D'H is supported in part by NSF Grants No. PHY-95-31023 and PHY-98-19686 and the research of D.Z.F by NSF Grant No. PHY-97-22072. J.E., who is a DFG Emmy Noether fellow, acknowledges funding through a DAAD postdoctoral fellowship. M.P.V. thanks MEC for a postdoctoral fellowship.

Appendix: AdS integrals

Here we study the integrals that appear in the calculation of near-extremal correlation functions via the AdS/CFT correspondence. We first give some explicit examples of integrals that appear in E_5^2 functions and then move to general properties of E_n^m integrals. We use the methods developed in [16], [35], [37] for general correlators and in [29] and [5] for extremal and next-to-extremal correlators. We use the Euclidean continuation of AdS_5 whose metric is given by

$$ds^2 = \frac{1}{z_0^2} (dz_0^2 + \sum_{i=1}^4 dz_i^2). \quad (\text{A.1})$$

The scalar bulk to boundary propagator is given by [3], [16]

$$K_\Delta(x, z) = C_\Delta \left(\frac{z_0}{z_0^2 + (\vec{z} - \vec{x})^2} \right)^\Delta, \quad C_\Delta = \frac{\Gamma(\Delta)}{\pi^2 \Gamma(\Delta - 2)}, \quad \Delta > 2,$$

$$C_2 = \frac{1}{2\pi^2}. \quad (\text{A.2})$$

$\Delta \geq 2$ is a real number. Divergences in AdS integrals can arise only when the integration points approach the boundary. Hence we need the behaviour of the propagators when the bulk point approaches the boundary. When $z_0 \rightarrow 0$ but $\vec{z} \not\rightarrow \vec{x}$,

$$K_\Delta(x, z) \rightarrow C_\Delta z_0^\Delta \frac{1}{(\vec{z} - \vec{x})^{2\Delta}}. \quad (\text{A.3})$$

On the other hand, when $z \rightarrow x$,

$$K_\Delta(x, z) \rightarrow z_0^{4-\Delta} \delta(\vec{z} - \vec{x}). \quad (\text{A.4})$$

The explicit form of the bulk propagator $G_\delta(y, z)$ is not needed here. Its behaviour when one of the points approaches the boundary is [35] [36], in the conventions of [15],

$$G_\delta(y, z) \xrightarrow{y_0 \rightarrow 0} \tilde{C}_\delta y_0^\delta K_\delta(\vec{y}, z), \quad \tilde{C}_\delta = \frac{2^{\delta-6}}{\delta-2} \frac{(2\pi)^5}{4N^2} \frac{(\delta+1)^2}{\delta(\delta-1)}, \quad k > 2, \\ \tilde{C}_2 = \frac{(2\pi)^5}{4N^2} \frac{9}{2^5}. \quad (\text{A.5})$$

Examples of five-point integrals

We first illustrate the general properties of AdS integrals by studying the contribution of diagram *b* of Fig. 3 to a general next-to-next-to-extremal five-point function. We always assume that the five points are non-coincident. The conformal dimensions of the chiral primary operators involved satisfy $\Delta = \sum_{i=1}^4 \Delta_i - 4$. We take ϕ and ϕ' to be chiral primaries of conformal dimension δ and δ' , respectively. The contribution of the diagram is

$$\langle \mathcal{O}_\Delta(x) \mathcal{O}_{\Delta_1}(x_1) \mathcal{O}_{\Delta_2}(x_2) \mathcal{O}_{\Delta_3}(x_3) \mathcal{O}_{\Delta_4}(x_4) \rangle \\ = \frac{\mathcal{G}_3(\Delta, \Delta_1, \delta) \mathcal{G}_3(\delta, \Delta_2, \delta') \mathcal{G}_3(\Delta_3, \Delta_4, \delta')}{\mathcal{N}_\Delta \mathcal{N}_{\Delta_1} \mathcal{N}_{\Delta_2} \mathcal{N}_{\Delta_3} \mathcal{N}_{\Delta_4}} \iiint \frac{d^5 y}{y_0^5} \frac{d^5 z}{z_0^5} \frac{d^5 w}{w_0^5} K_\Delta(x, y) K_{\Delta_1}(x_1, y) \\ \cdot G_\delta(y, z) K_{\Delta_2}(x_2, z) G_{\delta'}(z, w) K_{\Delta_3}(x_3, w) K_{\Delta_4}(x_4, w), \quad (\text{A.6})$$

with \mathcal{N}_Δ as in (2.12). The possible divergence can only arise from the region $y \sim x$. Indeed, in this region we can use Eqs. (A.3), (A.4) and (A.5) to see that the integrand is proportional to

$$y_0^{-5} y_0^{4-\Delta} y_0^{\Delta_1} y_0^\delta = y_0^{\delta+\Delta_1-\Delta-1} \\ \equiv y_0^{-\alpha-1} \quad (\text{A.7})$$

The degree of divergence of the integral over y_0 is given by α . The $SU(4)$ R-symmetry implies that $\delta \geq \Delta - \Delta_1$ and thus $\alpha \leq 0$. Hence there are two possibilities: the integral is

finite if $\alpha < 0$ and it is logarithmically divergent if $\alpha = 0$. Since $\Delta > \Delta_i$, $i = 1, \dots, 4$, a similar counting shows that the regions when one or more of the integration points approach any x_i do not give any divergence.

Let us consider first the divergent case which occurs when $\delta = \Delta - \Delta_1$. We regularize the integral by analytic continuation in the highest dimension which we write as $\Delta - \varepsilon$, $\varepsilon > 0$. The coupling of the vertex at y has to be changed accordingly. The integral is convergent since now we have $\alpha = -\varepsilon$. For small ε the integral is dominated by the contribution of the region $y \sim x$. In this region we can use Eq. (A.5) and write Eq. (A.6) as

$$\begin{aligned} & \langle \mathcal{O}_\Delta(x) \mathcal{O}_{\Delta_1}(x_1) \mathcal{O}_{\Delta_2}(x_2) \mathcal{O}_{\Delta_3}(x_3) \mathcal{O}_{\Delta_4}(x_4) \rangle_1 \\ &= I_1^y \cdot \langle \mathcal{O}_{\Delta-\Delta_1}(x) \mathcal{O}_{\Delta_2}(x_2) \mathcal{O}_{\Delta_3}(x_3) \mathcal{O}_{\Delta_4}(x_4) \rangle_1 \end{aligned} \quad (\text{A.8})$$

with

$$I_1^y = \mathcal{G}_3(\Delta - \varepsilon, \Delta_1, \delta) \frac{C_\Delta C_{\Delta_1} \tilde{C}_\delta}{(x - x_1)^{2\Delta_1}} \frac{\mathcal{N}_{\Delta-\Delta_1}}{\mathcal{N}_\Delta \mathcal{N}_{\Delta_1}} \int_{\mathcal{R}} \frac{d^5 y}{y_0^5} \frac{y_0^{2\Delta-\varepsilon}}{(y-x)^{2(\Delta-\varepsilon)}}, \quad (\text{A.9})$$

$$\begin{aligned} & \langle \mathcal{O}_{\Delta-\Delta_1}(x) \mathcal{O}_{\Delta_2}(x_2) \mathcal{O}_{\Delta_3}(x_3) \mathcal{O}_{\Delta_4}(x_4) \rangle_1 \\ &= (\mathcal{N}_{\Delta-\Delta_1} \mathcal{N}_{\Delta_2} \mathcal{N}_{\Delta_3} \mathcal{N}_{\Delta_4})^{-1} \mathcal{G}_3(\delta, \Delta_2, \delta') \mathcal{G}_3(\Delta_3, \Delta_4, \delta') \\ & \cdot \iint \frac{d^5 z}{z_0^5} \frac{d^5 w}{w_0^5} K_\delta(x, z) K_{\Delta_2}(x_2, z) G_{\delta'}(z, w) K_{\Delta_3}(x_3, w) K_{\Delta_4}(x_4, w). \end{aligned} \quad (\text{A.10})$$

\mathcal{R} is any neighbourhood of x where the approximation (A.5) is valid. The integral in I_1^y leads to a pole in ε , which is cancelled by a factor of ε arising from $\mathcal{G}_3(\Delta - \varepsilon, \Delta_1, \delta)$. This is described in detail in [5]. The result when $\varepsilon \rightarrow 0$ is

$$I_1^y = \frac{1}{N} \sqrt{\Delta \Delta_1 (\Delta - \Delta_1)} \langle \mathcal{O}_{\Delta_1}(x) \mathcal{O}_{\Delta_1}(x_1) \rangle. \quad (\text{A.11})$$

On the other hand, $\langle \mathcal{O}_{\Delta-\Delta_1}(x) \mathcal{O}_{\Delta_2}(x_2) \mathcal{O}_{\Delta_3}(x_3) \mathcal{O}_{\Delta_4}(x_4) \rangle_1$ has the form of an exchange contribution to a four-point function which may be evaluated using the methods of [37]. We see that the five point function contribution (A.8) factors into a free-field two-point function times a four-point function contribution.

As an example of a convergent integral, let us consider the case when the dimension of the exchanged fields is $\delta = \Delta - \Delta_1 + 2$ and $\delta' = \Delta_3 + \Delta_4 - 2$. The integral is convergent since $\alpha = -2$. Indeed, in this simple case we can perform the integral over y and w explicitly using the methods of [37] and find

$$\begin{aligned} & \langle \mathcal{O}_\Delta(x) \mathcal{O}_{\Delta_1}(x_1) \mathcal{O}_{\Delta_2}(x_2) \mathcal{O}_{\Delta_3}(x_3) \mathcal{O}_{\Delta_4}(x_4) \rangle_2 \\ &= \mathcal{G}(\Delta, \Delta_1, \Delta - \Delta_1 + 2) \mathcal{G}(\Delta - \Delta_1 + 2, \Delta_2, \Delta_3 + \Delta_4 - 2) \mathcal{G}(\Delta_3 + \Delta_4 - 2, \Delta_3, \Delta_4) \\ & \cdot a_{\Delta_4-1} \frac{1}{(x_3 - x_4)^2} \sum_{k=\Delta-\Delta_1+1}^{\Delta-1} b_k \frac{1}{(x - x_1)^{2(\Delta-k)}} \\ & \cdot \int \frac{d^5 y}{y_0^5} K_k(x, y) K_{\Delta_1-\Delta+k}(x_1, y) K_{\Delta_2}(x_2, y) K_{\Delta_3-1}(x_3, y) K_{\Delta_4-1}(x_4, y), \end{aligned} \quad (\text{A.12})$$

with finite coefficients a_{Δ_4-1} , b_k . The remaining y -integral is finite for every term in the sum [38]. Therefore, since the second coupling is extremal and therefore vanishes, the whole contribution vanishes.

As a final example for a five-point function contribution we consider diagram b of Fig. 3,

$$\begin{aligned} & \langle \mathcal{O}_\Delta(x) \mathcal{O}_{\Delta_1}(x_1) \mathcal{O}_{\Delta_2}(x_2) \mathcal{O}_{\Delta_3}(x_3) \mathcal{O}_{\Delta_4}(x_4) \rangle_3 \\ &= \frac{\mathcal{G}_3(\Delta, \delta, \delta') \mathcal{G}_3(\Delta_1, \Delta_2, \delta) \mathcal{G}_3(\Delta_3, \Delta_4, \delta')}{\mathcal{N}_\Delta \mathcal{N}_{\Delta_1} \mathcal{N}_{\Delta_2} \mathcal{N}_{\Delta_3} \mathcal{N}_{\Delta_4}} \iiint \frac{d^5 y}{y_0^5} \frac{d^5 z}{z_0^5} \frac{d^5 w}{w_0^5} K_\Delta(x, y) G_\delta(y, z) \\ & \quad \cdot K_{\Delta_1}(x_1, z) K_{\Delta_2}(x_2, z) G_{\delta'}(y, w) K_{\Delta_3}(x_3, w) K_{\Delta_4}(x_4, w), \end{aligned} \quad (\text{A.13})$$

when $\delta = \Delta_1 + \Delta_2 - 2$ and $\delta' = \Delta_3 + \Delta_4 - 2$. Again the vertex at y is extremal, and the dominant contribution arises when $y \sim x$. For this case the limit (A.5) applies to both bulk-to-bulk propagators, such that the integral factors into

$$\begin{aligned} & \langle \mathcal{O}_\Delta(x) \mathcal{O}_{\Delta_1}(x_1) \mathcal{O}_{\Delta_2}(x_2) \mathcal{O}_{\Delta_3}(x_3) \mathcal{O}_{\Delta_4}(x_4) \rangle_3 \\ &= I_3^y \cdot \langle \mathcal{O}_{\Delta_1+\Delta_1-2}(x) \mathcal{O}_{\Delta_1}(x_1) \mathcal{O}_{\Delta_2}(x_2) \rangle \langle \mathcal{O}_{\Delta_3+\Delta_4-2}(x) \mathcal{O}_{\Delta_3}(x_3) \mathcal{O}_{\Delta_4}(x_4) \rangle, \end{aligned} \quad (\text{A.14})$$

where

$$I_3^y = \tilde{C}_{\Delta_1+\Delta_2-2} \tilde{C}_{\Delta_3+\Delta_4-2} C_\Delta \frac{\mathcal{N}_{\Delta_1+\Delta_2-2} \mathcal{N}_{\Delta_3+\Delta_4-2}}{\mathcal{N}_\Delta} \mathcal{G}(\Delta - \varepsilon, \delta, \delta') \int_{\mathcal{R}} \frac{d^5 y}{y_0^5} \frac{y_0^{2\Delta-\varepsilon}}{(y-x)^{2(\Delta-\varepsilon)}} \quad (\text{A.15})$$

and

$$\begin{aligned} & \langle \mathcal{O}_{\Delta_1+\Delta_1-2}(x) \mathcal{O}_{\Delta_1}(x_1) \mathcal{O}_{\Delta_2}(x_2) \rangle \\ &= \frac{\mathcal{G}(\delta, \Delta_1, \Delta_2)}{\mathcal{N}_{\Delta_1+\Delta_2-2} \mathcal{N}_{\Delta_1} \mathcal{N}_{\Delta_2}} \int \frac{d^5 w}{w_0^5} K_\delta(x, w) K_{\Delta_1}(x_1, w) K_{\Delta_2}(x_2, w) \\ &= \frac{1}{N} \frac{\sqrt{(\Delta_1 + \Delta_2 - 2) \Delta_1 \Delta_2}}{(x-x_1)^{2(\Delta_1-1)} (x-x_2)^{2(\Delta_2-1)} (x_1-x_2)^2}, \end{aligned} \quad (\text{A.16})$$

such that we obtain

$$\begin{aligned} & \langle \mathcal{O}_\Delta(x) \mathcal{O}_{\Delta_1}(x_1) \mathcal{O}_{\Delta_2}(x_2) \mathcal{O}_{\Delta_3}(x_3) \mathcal{O}_{\Delta_4}(x_4) \rangle_3 \\ &= \frac{1}{N} \sqrt{\Delta(\Delta_1 + \Delta_2 - 2)(\Delta_3 + \Delta_4 - 2)} \langle \mathcal{O}_{\Delta_1+\Delta_1-2}(x) \mathcal{O}_{\Delta_1}(x_1) \mathcal{O}_{\Delta_2}(x_2) \rangle \\ & \quad \cdot \langle \mathcal{O}_{\Delta_3+\Delta_4-2}(x) \mathcal{O}_{\Delta_3}(x_3) \mathcal{O}_{\Delta_4}(x_4) \rangle \end{aligned} \quad (\text{A.17})$$

which agrees exactly with the corresponding contribution to the field theory result (3.10).

General AdS integrals

Let us now turn to studying general E_{n+1}^m functions with $m \leq n - 2$ (and non-coincident points). This is relevant for the inductive proof of Section 5. For simplicity we work

with non-derivative couplings. Derivative couplings do not change the leading degree of divergence of the integrals: if y is the integration variable, the derivatives $\partial/\partial y_0$ make the integrand more singular as y approach the boundary, but this effect is exactly compensated by the powers of y_0 arising from the metric. On the other hand, we assume in the following that all the extremal couplings vanish. More precisely, if analytic continuation is used, we assume that the extremal couplings contains a zero in the regulator. This is required in order to obtain non-divergent Witten diagrams. We consider first the contact diagram (diagram a in Fig. 11) and regularize a possible divergence by analytical continuation in the highest dimension, Δ . This does not affect the result if the integral is convergent. Up to couplings the diagram gives

$$\mathcal{I}_a = \int \frac{d^5 y}{y_0^5} K_{\Delta-\varepsilon}(x, y) \prod_{i=1}^n K_{\Delta_i}(x_i, y). \quad (\text{A.18})$$

As $y \rightarrow x$ the integrand is proportional to $y_0^{\sum_i \Delta_i - (\Delta - \varepsilon) - 1}$, *i.e.*, $\alpha = \Delta - \varepsilon - \sum_i \Delta_i$ for this diagram. Therefore, for $\varepsilon = 0$ the integral diverges logarithmically if the function is extremal and is convergent in any sub-extremal case. Obviously the integrand is less singular in the regions $y \sim x_i$, as the m -extremality condition implies that $\Delta_i < \Delta$. In the extremal case, $\Delta = \sum_i \Delta_i$, the integral gives rise to a pole in ε arising from the region $y \sim x$:

$$\begin{aligned} \mathcal{I}_a &\sim \int_{\mathcal{R}} \frac{dy_0}{y_0} y_0^\varepsilon \prod_{i=1}^n \frac{1}{(x - x_i)^{2\Delta_i}} + R_a \\ &\sim \frac{1}{\varepsilon} \prod_{i=1}^n \frac{1}{(x - x_i)^{2\Delta_i}} + R'_a, \end{aligned} \quad (\text{A.19})$$

where R_a and R'_a are analytic in ε . The pole is cancelled by a zero in the extremal coupling. Hence, the analytic part R' is irrelevant when $\varepsilon \rightarrow 0$, and the diagram factors into n two-point functions.

A typical exchange diagram is shown in Fig. 13. Let us study the possible divergent limits. We consider first the case when only one internal point, which we denote generically as u , approaches a point x' in the boundary. If $x' \neq x_i$, $i = 0, \dots, 9$ ($x_0 \equiv x$) or $x' = x_i$ but u is not directly connected to x_i by a bulk-to-boundary propagator, both the bulk propagators and bulk-to-boundary propagators connected to u are proportional to positive powers of u_0 as $u_0 \rightarrow 0$. For example, if $y \rightarrow x_2$, the integrand is proportional to $y_0^{\Delta + \Delta_1 + \delta_1 + \delta_2 - 5}$. In the worst possible case the integrand is proportional to $u_0^{2+2+2-5}$. Hence this region does not contribute to the integral. On the other hand, if $x' = x_i$ and u is directly connected to x_i there is a power $u_0^{4-\Delta_i}$. For instance, if $y \rightarrow x$ the integrand is proportional to $y_0^{\Delta_1 + \delta_1 + \delta_2 - \Delta - 1}$. Therefore a logarithmic divergence appears in this region if the vertex at u is extremal and Δ_i is the largest dimension entering this vertex. Otherwise the integral over this region is finite. For instance, if $y \rightarrow x$ the integrand is proportional to $y_0^{\Delta_1 + \delta_1 + \delta_2 - \Delta - 1}$.

Let us now allow the possibility that two bulk points u_1 and u_2 approach the boundary. If they approach different points the two limits can be considered independently. For instance,

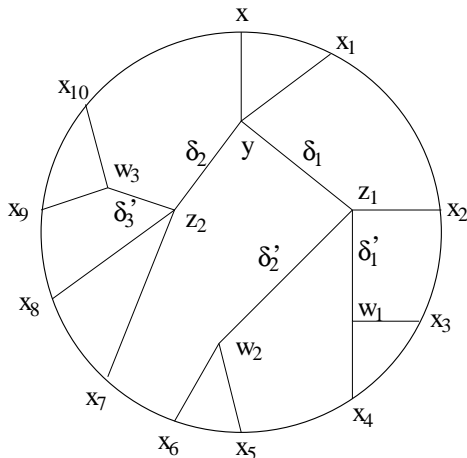


Figure 13: Typical exchange diagram.

if $y \rightarrow x$ and $z_1 \rightarrow x_2$, the integrand is proportional to $y_0^{\Delta_1 + \delta_1 + \delta_2 - \Delta - 1} (z_1)_0^{\delta_1 + \delta_1' + \delta_2' - \Delta_2 - 1}$. If u_1 and u_2 approach the same point x' and none of them is directly connected to this point, all the propagators contribute with positive powers of $(u_1)_0$ and $(u_2)_0$ and the double integral over u_1 and u_2 is convergent. Finally, if $u_1 \rightarrow x_i$ and $u_2 \rightarrow x_i$ and x_i is directly connected to, say, u_1 , there are two possibilities: If u_1 and u_2 are not directly connected by a bulk propagator there is a factor of $(u_1)_0^{4 - \Delta_i}$ but all the powers of $(u_2)_0$ are positive. On the other hand, if u_1 and u_2 are directly connected there are two factors with negative powers: $(u_1)_0^{4 - \Delta_i} (u_2)_0^{4 - \delta_{12}}$, where δ_{12} is the dimension of the propagator connecting u_1 and u_2 . For example, if $y \rightarrow x$ and $z_2 \rightarrow x$, the integrand is proportional to $y_0^{\Delta_1 + \delta_1 + \delta_2 - \Delta - 1} (z_2)_0^{\Delta_6 + \Delta_7 + \Delta_8' - \delta_2 - 1}$. The integral over y (z_2) is then logarithmically divergent if the vertex at y (z_2) is extremal. In general, a (logarithmic) divergence in the integral over an internal point u can only arise when the following two conditions are fulfilled:

1. Either u approaches a point x_i that is connected to u by a bulk-to-boundary propagator or it approaches a point x_i that is connected to u by a string of propagators and all the points in those propagators also approach x_i .
2. The vertex at u is extremal and the highest dimension of the fields entering the vertex is the one of the field that connects u (directly or indirectly) with x_i .

We shall use these properties in the following.

Any diagram with at least one exchange is of the general form represented by diagram b of Fig. 11, where we have isolated the vertex at y to which the highest-dimension operator is connected. This vertex involves $(k_0 + 1)$ bulk-to-boundary propagators and r bulk-to-bulk propagators depending on y and one z_j , $j = 1, \dots, r$. There are r subdiagrams involving further tree interactions depicted by a shadowed circle. The j th subdiagram

depends on the bulk variable z_j and on k_j boundary variables $x_{k_0+\dots+k_{j-1}+1}, \dots, x_{k_0+\dots+k_j}$ which we collectively denote as \tilde{x}_j . We denote the contribution from the j th subdiagram by $D_j(z_j, \tilde{x}_j)$. Using analytic continuation, the contribution of diagram b is given by

$$\mathcal{I}_b = \int \frac{d^5 y}{y_0^5} K_{\Delta-\varepsilon}(x, y) \prod_{i=1}^k K_{\Delta_i}(x_i, y) \prod_{j=1}^r \int \frac{d^5 z_j}{(z_j)_0^5} G_{\delta_j}(y, z_j) D_j(z_j, \tilde{x}_j), \quad (\text{A.20})$$

where we have omitted the couplings. A divergence in the integral over y can only arise from the region $y \sim x$. The degree of divergence is given by

$$\alpha = \Delta - \sum_{i=1}^k \Delta_i - \sum_{j=1}^r \delta_j - \varepsilon. \quad (\text{A.21})$$

Therefore the integral over y is divergent (for $\varepsilon = 0$) if and only if the vertex at y is extremal, $\sum_{j=1}^r \delta_j = \Delta - \sum_{i=1}^k \Delta_i$. In this case (*case (1)* in the text), the integral is dominated by the region $y \sim x$ which gives rise to a pole $1/\varepsilon$:

$$\mathcal{I}_b \sim \int_{\mathcal{R}} \frac{dy_0}{y_0} y_0^\varepsilon \prod_{i=1}^k \frac{1}{(x-x_i)^{\Delta_i}} \prod_{j=1}^r \int \frac{d^5 z_j}{(z_j)_0^5} K_{\delta_j}(x, z_j) D_j(z_j, \tilde{x}_j) + R_b \quad (\text{A.22})$$

$$\sim \frac{1}{\varepsilon} \prod_{i=1}^k \frac{1}{(x-x_i)^{\Delta_i}} \prod_{j=1}^r H_j(x, \tilde{x}_j) + R'_b, \quad (\text{A.23})$$

where R_b and R'_b are regular in ε and

$$H_j(x, \tilde{x}_j) \equiv \int \frac{d^5 z_j}{(z_j)_0^5} K_{\delta_j}(x, z_j) D_j(z_j, \tilde{x}_j). \quad (\text{A.24})$$

Since the extremal coupling contains a factor of ε , the final result is finite and factors into k two-point functions times a product of r functions. The j th of these functions has $k_j + 1$ points. This structure is illustrated in Fig. 12.

Consider now the case when the vertex at y is sub-extremal: $\sum_{j=1}^r \delta_j > \Delta - \sum_{i=1}^k \Delta_i$. Then we have $\alpha < 0$ (we set $\varepsilon = 0$ now) and the integral over y is convergent. We also have to study the behaviour of the integrand when some of the other internal points approach the boundary. As we have shown above, (logarithmic) divergences only arise from extremal vertices. They manifest as poles in analytic continuation and are cancelled by the zeros in the corresponding extremal couplings. The diagram is then finite even if the coupling of the vertex at y is not included. Therefore if this coupling vanishes, as in *case (2)* in the text, the diagram gives zero. Finally, for *case (3)* in the text we need to show that the diagram vanishes when one of the subdiagrams is an $\tilde{E}_{k_j+1}^p$ function (*i.e.*, an $E_{k_j+1}^p$ function with the bulk-to-boundary propagator of highest dimension changed by a bulk propagator) and $p \leq k_j - 2$. This subdiagram can be either contact or exchange (diagrams a and b of Fig. 14). The power counting shows that the integral over z_j in the contact diagram is convergent. This is all we need for diagram a . In diagram b we can distinguish again two possibilities:

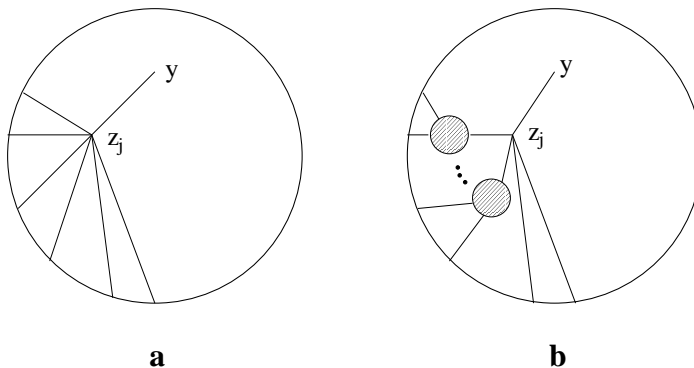


Figure 14: Contact (a) and exchange (b) contributions to a subdiagram of the exchange diagram in Fig. 10.

1. If the vertex at z_j is extremal with δ_j the highest dimension, according to the analysis above one can only have a logarithmic divergence in the integration over z_j when $y \rightarrow x$ and $z_j \rightarrow x$. The behaviour of the integrand is then

$$y_0^{\left(\sum_{l=1}^r \delta_l + \sum_{i=1}^k \Delta_i - \Delta - 1 - \varepsilon'\right)} (z_j)_0^{\varepsilon' - 1},$$

where ε' is a regulator of the z_j integral. The $1/\varepsilon'$ pole in the z_j integral is cancelled by a ε' factor in the corresponding extremal coupling. Moreover, as the vertex at y is sub-extremal the region $y \sim x$ of the integral over y gives a vanishing contribution. Therefore, the region $y \sim x, z \sim x$ does not contribute to diagram *b*. On the other hand if y is away from x there is no divergence in the z_j integral, and the zero in the coupling ensures that the diagram vanishes.

2. If the vertex at z_j is sub-extremal, the integral over z_j converges. The divergences in the remaining integrals are cancelled by zeros in the corresponding couplings. Therefore the diagram vanishes if the coupling of the vertex at z_j vanishes. As we show in the text, if this coupling does not vanish the subdiagram contains at least one (non-trivial) subdiagram that is a an $\tilde{E}_{k'_j+1}^m$ function with $m \leq k'_j - 2$ and the same procedure can be employed to analyze it.

The iteration ends when the last \tilde{E} function is a contact diagram.

References

- [1] J. Maldacena, Adv. Theor. Math. Phys. **2**, 231 (1998), hep-th/9711200.

- [2] S.S. Gubser, I.R. Klebanov and A.M. Polyakov, Phys. Lett. **B428**, 105 (1998), hep-th/9802109.
- [3] E. Witten, Adv. Theor. Math. Phys. **2**, 253 (1998), hep-th/9802150.
- [4] M. Bianchi and S. Kovacs, Phys. Lett. **B468**, 102 (1999), hep-th/9910016.
- [5] J. Erdmenger and M. Pérez-Victoria, “Non-renormalization of next-to-extremal correlators in $\mathcal{N} = 4$ SYM and the AdS/CFT correspondence”, hep-th/9912250, to be published in Phys. Rev. **D**.
- [6] G. Arutyunov and S. Frolov, “On the correspondence between gravity fields and CFT operators”, hep-th/0003038.
- [7] F. Gonzalez-Rey, I.Y. Park and K. Schalm, Phys. Lett. **B448**, 37 (1999), hep-th/9811155.
- [8] B. Eden, P. S. Howe, C. Schubert, E. Sokatchev and P. C. West, Nucl. Phys. **B557**, 355 (1999), hep-th/9811172.
- [9] B. Eden, C. Schubert and E. Sokatchev, “Three-loop four-point correlator in $N = 4$ SYM”, hep-th/0003096.
- [10] G. Arutyunov and S. Frolov, “Four-point functions of lowest weight CPOs in $N = 4$ SYM(4) in supergravity approximation”, hep-th/0002170.
- [11] L. Hoffmann, A. C. Petkou and W. Rühl, “Aspects of the conformal operator product expansion in AdS/CFT correspondence”, hep-th/0002154.
- [12] G. Chalmers and K. Schalm, Nucl. Phys. **B554**, 215 (1999), hep-th/9810051.
- [13] M. Gunaydin, L. J. Romans and N. P. Warner, Phys. Lett. **B154**, 268 (1985).
- [14] M. Pernici, K. Pilch and P. van Nieuwenhuizen, Nucl. Phys. **B259**, 460 (1985).
- [15] S. Lee, S. Minwalla, M. Rangamani and N. Seiberg, Adv. Theor. Math. Phys. **2**, 697 (1998), hep-th/9806074.
- [16] D. Z. Freedman, S. D. Mathur, A. Matusis and L. Rastelli, Nucl. Phys. **B546**, 96 (1999), hep-th/9804058.
- [17] E. D’Hoker, D.Z. Freedman and W. Skiba, Phys. Rev. **D59**, 045008 (1999), hep-th/9807098.
- [18] F. Gonzalez-Rey, B. Kulik and I.Y. Park, Phys. Lett. **B455**, 164 (1999), hep-th/9903094.
- [19] S. Penati, A. Santambrogio and D. Zanon, JHEP **9912**, 006 (1999), hep-th/9910197.

- [20] B. Eden, P. S. Howe and P. C. West, Phys. Lett. **B463**, 19 (1999), hep-th/9905085.
- [21] P. S. Howe, C. Schubert, E. Sokatchev and P. C. West, “Explicit construction of nilpotent covariants in $N = 4$ SYM”, hep-th/9910011.
- [22] K. Intriligator, Nucl. Phys. **B551**, 575 (1999), hep-th/9811047.
- [23] A. Petkou and K. Skenderis, Nucl. Phys. **B561**, 100 (1999), hep-th/9906030.
- [24] S. Ferrara and E. Sokatchev, “Short representations of $SU(2,2/N)$ and harmonic superspace analyticity”, hep-th/9912168.
- [25] V. K. Dobrev and V. B. Petkova, Lett. Math. Phys. **9**, 287 (1985).
- [26] W. Skiba, Phys. Rev. **D60**, 105038 (1999), hep-th/9907088.
- [27] M. Bianchi, S. Kovacs, G. Rossi and Y. S. Stanev, JHEP **9908**, 020 (1999), hep-th/9906188.
- [28] M. Bianchi, S. Kovacs, G. Rossi and Y. S. Stanev, “Anomalous dimensions in $\mathcal{N} = 4$ SYM theory at order g^4 ”, hep-th/0003203.
- [29] E. D’Hoker, D.Z. Freedman, S. Mathur, A. Matusis and L. Rastelli, “Extremal correlators in the AdS/CFT correspondence”, hep-th/9908160.
- [30] B. Eden, P.S. Howe, C. Schubert, E. Sokatchev and P.C. West, Phys. Lett. **B472**, 323 (2000), hep-th/9910150.
- [31] G. Arutyunov and S. Frolov, Phys. Rev. **D61**, 064009 (2000), hep-th/9907085.
- [32] S. Lee, “AdS(5)/CFT(4) four-point functions of chiral primary operators: Cubic vertices”, hep-th/9907108.
- [33] G. Arutyunov and S. Frolov, “Scalar Quartic Couplings in Type II B Supergravity on $AdS_5 \times S^5$ ”, hep-th/9912210.
- [34] I. Klebanov and E. Witten, Nucl. Phys. **B556**, 89 (1999), hep-th/9905104.
- [35] E. D’Hoker and D. Z. Freedman, Nucl. Phys. **B550**, 261 (1999), hep-th/9811257.
- [36] E. D’Hoker, S. D. Mathur, A. Matusis and L. Rastelli, “The operator product expansion of $N = 4$ SYM and the 4-point functions of supergravity”, hep-th/9911222.
- [37] E. D’Hoker, D. Z. Freedman and L. Rastelli, Nucl. Phys. **B562**, 395 (1999), hep-th/9905049.
- [38] E. D’Hoker, D. Z. Freedman, S. D. Mathur, A. Matusis and L. Rastelli, Nucl. Phys. **B562**, 353 (1999), hep-th/9903196.